People's Democratic Republic of Algeria Ministry of Higher Education and Scientific Research

Echahid Hamma Lakhdar University of El-Oued

FACULTY OF TECHNOLOGY

MECHANICAL ENGINEERING DEPARTMENT

End of study thesis

Presented for the graduation of

ACADEMIC MASTER

Field: Technologies
Sector: Mechanical engineering
Specialty: Renewable Energies

Theme:

The effect of temperature on the properties of NiO thin layers produced by solar pyrolysis spray

Before the jury composed of:

Dr. Khaled Miloudi	President
Dr. Mohammed Khachana	Examiner
Dr. Yacine Aoun	Supervisor
Dr. Abdelbaki Nid	Co-Supervisor

Presented by:

- Zakaria Dou
- Oussama Debbab
- Sad Bousbia Laiche

2020-2021

Acknowledgement

We thank, Allah the Almighty for giving us the will and patience to carry out this modest work.

We would like to express our warm thanks to our mentor Dr. Yacine AOUN for his support, guidance and advice which were very precious to us.

We cannot forget to thank also Mr. President and Gentlemen of the jury, also all the staff of the Faculties of Technology and Exact Sciences of the Echahid Hamma Lakhdar University of El-Oued, in particular

We extend our acknowledgment to Abdelbaki Nid for wise word of advice.

Also, we thanks My School work team for various assistance and support

Dedication

Our dedication goes to our beloved parents, who have been along us through the road leading to this moment.

Thank you.

Table of Content

Chapter III: Results and Discussion

List of Figures

Chapter I: General Information on Solar Energy and NiO Thin Films

Chapter II: Techniques for Elaboration and characterization devices for (NiO) thin films

Chapter III: Results and Discussion

List of Tables

Abbreviation

Notation	Unites
TCO: Transparent Conductive Oxides	
NiO: Nickel oxide	
PTC: Parabolic trough collectors	
HFC: Heliostat field collector	
CLFR: Concentrating linear Fresnel reflector	
PDC: Parabolic dish concentrators	
ALD: Atomic Layer Deposition	
TN: Néel temperature	
ALE: Atomic Layer Epitaxy	
CBD: Chemical Bath Deposition	
LPE: Liquid Phase Epitaxy	
IBAD: Ion Beam Assisted Deposition	
BLT: Boundary Layer Theory	
SPT: Spray Pyrolysis Technique	
XRD: X-Ray Diffraction	
UV: Ultraviolet	
FWHM: Full Width at Half Maximum	
PVD: Physical Vapor Deposition	
CVD: Chemical Vapor Deposition	
σ: Electrical conductivity	$[\Omega^{-1}cm^{-1}]$
Eg: Band gap energy (optical gap)	[eV]
ε: Dielectric constant	[F / m]
dhkl: Inter-reticular distance	[Å]
a: Mesh parameter	[Å]
θ: Angle of incidence (angle of reflection)	[degree]
λ: Wavelength of incident X photons	[Å]
n: Order of diffraction	(whole number)
D: Size of crystallites	[nm]

α: Absorption coefficient	[m-1]
h: Planck constant is 6,63.10-34	[J.s]
v: Wave frequency	[Hz]
Eu: Urbach energy	[J]
Rs: Surface resistance	[Ω]
ρ: Electrical resistivity	[Ω.cm]
I: Current intensity	[A]
U: Current voltage	[V]
T: Transmittance	[%]
t: Thickness	[nm]
n: $materialquantity$	[mole]
m: $Mass$	[g]
M: $Molarmass$	[g/mole]
C: $concentration$	[mole/l]
V: $volume$	[ml]

General Introduction

General Introduction

Solar energy is considered among the most important branches of renewable energies due to the availability of its main source “the sun” all over the world, which led to the spread of the use of solar energy in most countries. Among these types of Parabolic dish concentrators, which in turn have multiple uses, for example, the production of thin films.

Transparent and conductive oxides (TCO) are amazing materials in many ways. Their dual property, electrical conductivity and apparent transparency, makes them great candidates for use in optoelectronics, photovoltaics, and electrochromic windows [80].

Other uses for TCO include optical sensors, transparent electrical contacts in solar cells, flat screens, liquid crystal displays, and touch screens [81].

The usage of thin films is particularly appealing in industries where downsizing and low dimensionality of devices are required, such as the microelectronics industry [82].

Among these materials, nickel oxides (NiO) have received a lot of attention because of their good electrochemical stability and electrocatalytic activity, as well as their low cost for extended applications, with potential applications in various technologies such as Li+ batteries, super capacitors, gas sensors, photocatalysts, and Electrochromic materials. Furthermore, NiO has been reported to be a promising semiconductor for optoelectronic devices [80].

The aim of this thesis is to apply the pyrolysis spray process for manufacture of nickel oxide films and to investigate the effect of changing of tempeaurtes on the structural, optical, and electrical properties of these films by using parabolic dish concentrators solar.

After a general introduction, the dissertation is structured as follows:

The first chapter first includes a few different deposition processes that currently allow thin films to be obtained, and then we present the principle of deposit growth and the various substrate heating methods.

The second chapter is devoted to the thin films of nickel oxide in particular (their crystallographic, optical and electrical properties) with some applications, as well as the method of production and heating used.

The thin layers of NiO were deposited by the spray technique from a solution of nickel nitrate. The films were deposited on glass substrates heated using a solar oven. After that, we talked about the different characterization techniques used to analyze and determine the different structural, optical and electrical properties of thin layers produced from NiO (1.DRX, 2.Spectroscopy UV-visible, 3.Technique des quatre points) is presented. ..).

Chapter Three brings together the characterization results we obtained in our layers and

discussions on the results obtained during this study.

Finally, a general conclusion outlining the essence of the research work carried out as well as the prospects.

Chapter I

General Information on Solar Energy and NiO Thin Films

Chapter I: General Information on Solar Energy and NiO Thin Films

I.1. Introduction

The energy industry is expanding every year, so research on another new energy source, specifically renewable energies, and particularly solar energy, is required. Solar energy is obtained from the sun and can be represented by two systems: solar thermal systems (heat) such as solar thermal collectors and solar photovoltaic systems (electricity) such as solar photovoltaic collectors (solar panel). This research is interested in the thermal utilization of solar energy utilizing a parabolic solar collector in this work.

In addition, in this chapter we are going to discusses generalities regarding thin films before citing specific techniques of their physical and chemical deposits, as well as the features of the chosen substances. Finally, this chapter exposes the spray pyrolysis process.

I.2. Solar Energy

I.2.1. The Sun

Our solar system revolves around the sun, which is the central star. It's primarily hydrogen, which makes up roughly three-quarters of its overall mass, and helium, which makes up roughly a quarter of its total mass. [1] The rest of its bulk is made up of other elements that are present in considerably lesser quantities and account for little under 2% of the sun's mass.

Carbon, nitrogen, oxygen, neon, magnesium, silicon, sulfur, and iron are among these elements. In trace concentrations, over 50 additional elements can be discovered. The surface of the Sun has a temperature of 5778 K (5505°C). [2]

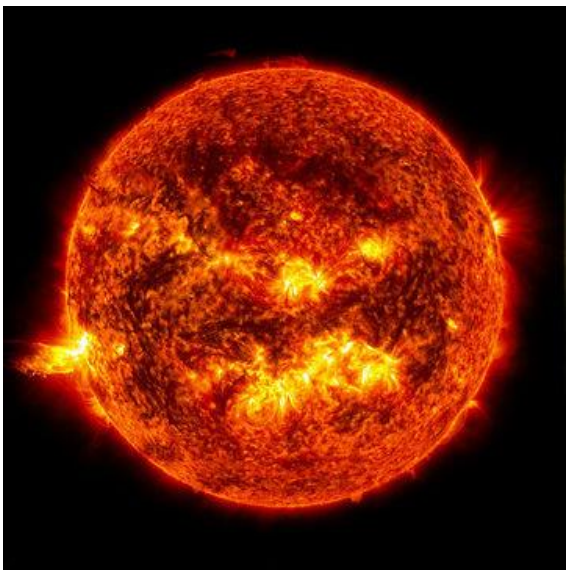

Figure I. 1: An image of the Sun [3].

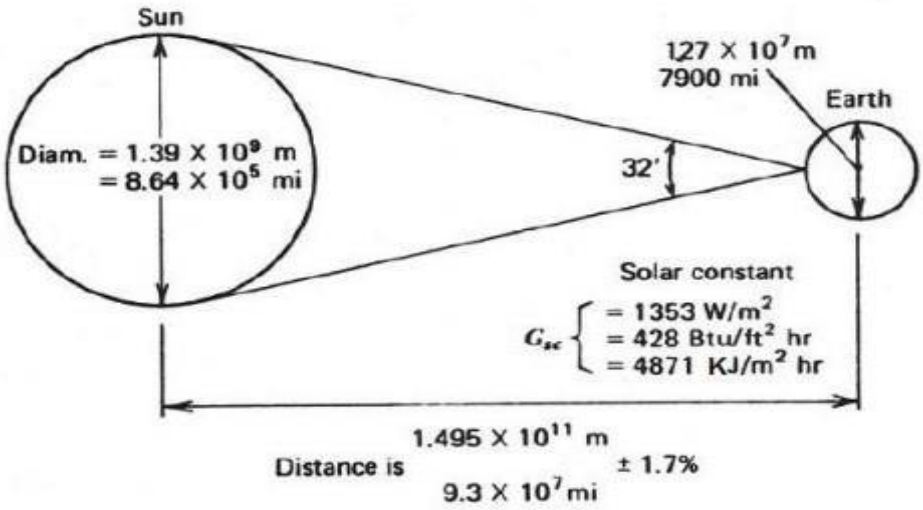

Figure I. 2: Sun - Earth relationship.

Only a modified proportion of solar energy reaches the earth's surface after being absorbed and diluted by entering the atmosphere, consisting of three main forms of radiation:

- Direct Radiation: solar radiation received directly. A pyrheliometer can be used to measure it.
- Diffused Radiation: a type of radiation that comes from the entire sky. This radiation is caused by the atmosphere's absorption and dispersion of solar energy, as well as its reflection by clouds. A pyranometer with a sun-masking screen can be used to measure it.
- Reflected Solar Radiation, often known as the ground's albedo, is the radiation reflected by the ground or objects on its surface. When the ground is exceptionally reflective, this albedo might be critical (water, snow).

I.2.2. Energy from the Sun

The Sun's energy is essential for life on the planet. It not only allows life to persist, but it is also the origin of the majority of energy used by mankind. The Sun is the source of biomass, fossil fuels, and other renewable energy like wind and solar electricity. Solar power is merely preserved as a secondary form in fossil fuels. [4] Photosynthesis captures the Sun's initial energy and preserves it in chemical bonds as plants flourish. After these plants have changed into fossil fuels, this energy is emitted millions of years later. All fossil fuels are fundamentally composed of sunlight-derived energy. Even after traversing through hundreds of miles on Earth's atmosphere, solar radiation finally reaches the planet, carrying a considerable quantity of energy. Generally, the solar power reaching Earth at the surface of the higher layer of the atmosphere is about 1367 W/m2 at full intensity. [5] The power output is approximately 340

W/m2, taking into consideration the fact that only half of the Earth faces the Sun, as well as the varying quantities of sunlight that strike various latitudes and the volume of atmosphere that the sunrays need to travel through.

The energy of the sun not only produces power, but it also heats the Earth to a habitable temperature degree (the structure of the atmosphere also contributes to Earth's energy quota maintaining a steady, sustainable temperature). Weather patterns as well as ocean and air currents are all caused by the Sun. [4]

I.2.3. The Solar Deposit in Algeria

Algeria covers more than 2.3 million square kilometers, with the Sahara accounting for 80% and 20% of the combined area of the African Sahara, respectively. This is a significant advantage for the country because it has a large stock of solar energy, which is considered one of the world's largest reserves, with sunshine lasting more than 3000 hours per year.

Table I. 1: shows the distribution of solar energy concentrations in Algeria.

Area	Coastal Area	High plateaus	Desert
Surface	4%	10%	86%
Average duration of sunning (h/ year)	2659	3000	3500
Average energy obtained (kwh/m2/year)	1700	1900	2650

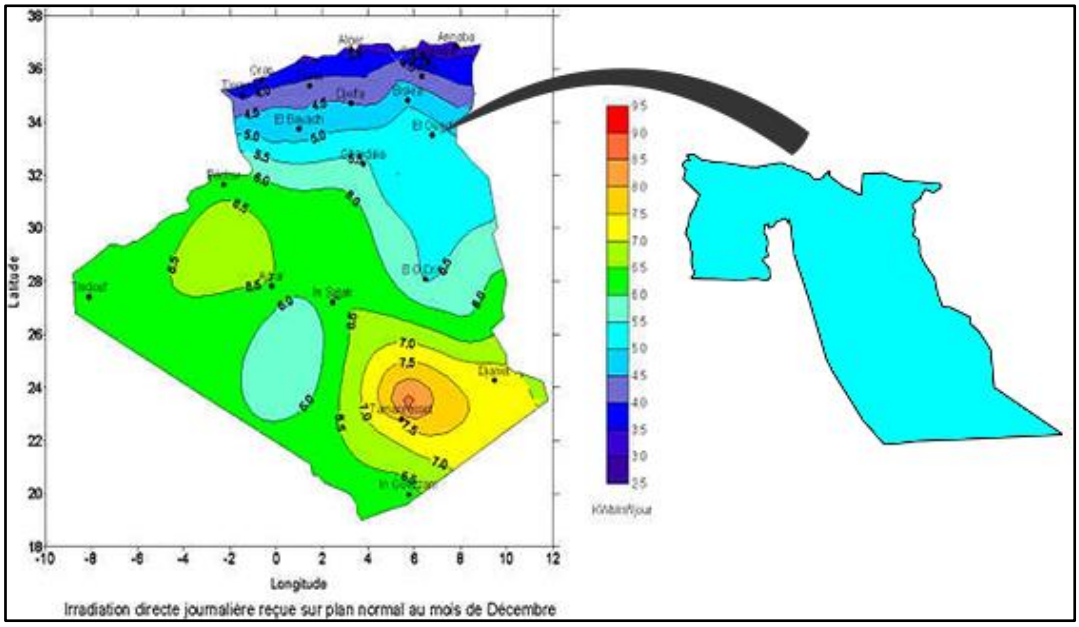

Figure I. 3: The Algerian solar map [7].

In Hassi, Algeria, a hybrid power plant has been built. The first of its sort in the world, Al-Raml, is powered by a combination of gas and solar energy, with a capacity of 150 megawatts, while the other is in Ghardaia, with a capacity of 1.1 megawatts.

As well, Willayet El-Oued is one of the most important places in Algeria because of the long day and high temperature that can reach. Also, most of the year is sunny and clear.

I.2.4. Uses of the solar energy

Solar water heating, solar building heating, solar distillation, solar pumping, solar drying of agricultural and animal products, solar furnaces, solar cooking, solar electric power generation, solar thermal power production, and solar green houses are just a few of the many applications of solar energy.

a) Solar Water Heating

A blackened flat plate metal collector and metal tubing, facing the general direction of the sun, are what constitute a solar water-heating system. A clear glass cover sits above the plate collector, with a layer of heat insulation underneath it.

b) Solar Heating of Buildings

c) Solar-distillation

Solar water distillation is the process of separating freshwater from salts or other impurities using energy from the sun. Untreated water absorbs heat and gradually rises to high temperatures. Water evaporates, cools, and condenses into vapour as a result of the heat, leaving

the impurities behind. Solar stills can be used to power low-capacity and self-sufficient water-supply systems. [8]

d) Solar-pumping

The electricity generated by solar energy is used to pump water for irrigation purposes in solar pumping. The need for water pumping is greatest during the hot summer months, which coincide with higher solar radiation, and hence this approach is best suited for irrigation. During periods of inclement weather, when solar radiations are low, the need for water pumping is also reduced since crop transpiration losses are low.

e) Solar Drying of Agricultural and Animal Products

Since the dawn of civilization, solar drying has been used to dry agricultural stocks as well as other goods. Traditional methods, although inexpensive, often produce poorer qualities of goods, in which hygiene cannot be guaranteed. Using the latest technologies, major improvements in sun drying can be accomplished. Solar energy has long been used to dry a variety of vegetables and fruits, palm nuts, copra, soya bean, meat, and fish. The systematic application of modern solar drying to carefully selected, high-value commodities for export or consumption by affluent people should result in clean and refined materials, significant weight reduction, and enhanced preservation and flavor. These elements can have a significant impact on marketing. [9]

f) Solar Furnaces

High temperatures are generated in a solar furnace by concentrating sun radiations onto a specimen using a number of heliostats (turnable mirrors) positioned on a sloping surface. The sun furnace is used to research the properties of ceramics at extremely high temperatures that beyond the range detectable in laboratories using flames and electric currents.

Heating can be done without contaminating the item in focus, and temperature can be easily regulated by shifting the position of the substance in focus. This is particularly beneficial in metallurgical and chemical activities. On an open specimen, many property measurements are available. The manufacture of nitric acid and fertilizers from air is an important potential application of solar furnaces.

g) Solar Cooking

Solar cooking is the use of direct sunlight energy to cook and heat food. The concept of utilizing heat from sunshine dates back to Archimedes of Syracuse's time in the Classical World. The sun is a never-ending source of energy for humanity. [10]

h) Solar Electric Power Generation

Photovoltaic cells may directly produce electric energy or electricity from solar energy. The photovoltaic cell is an energy conversion device that converts solar photons directly into electricity. It is built of semi-conductors, which absorb photons from the sun and produce free electrons with high energies.

i) Solar Thermal Power Production

Solar thermal power generation is the process of converting solar energy into electricity via thermal energy. Solar radiation is first used in this technique to heat up a working fluid, gas, water, or any other volatile liquid. This thermal energy is subsequently transformed into mechanical energy through the use of a turbine. Finally, mechanical energy is converted into electrical energy via a standard generator linked to a turbine. In countries with abundant sunshine, such as Algeria, thermodynamic solar energy is effective.

Among the techniques employed in this category are:

- Parabolic trough collectors (PTC)
- Heliostat field collector (HFC)
- Concentrating linear Fresnel reflector (CLFR)
- Parabolic dish concentrators (PDC)

Parabolic dish concentrators (PDC)

The parabolic geometry of this device makes it possible to concentrate all of the light rays which fall on the surface of the dish at a point where the baking dish is placed. The power of this device depends of course on the size of the dish; with a parabola 1.4 meters in diameter, several liters of water can be boiled in 30 minutes; the largest parabolas allow temperatures of around 800 degrees to be reached (solar oven in the Pyrénées Orientales). It is more dangerous to use because it reaches high temperatures. Devices whose focus is outside the parabola are dangerous because the power available at this focus quickly reaches a few hundred watts: this can for example cause serious lesions in the eye or is at the origin of a fire.

Since our study requires high temperatures above 300 ° C, we will therefore study a solar oven in parabolic form and subsequently manage to use it.

This study uses the Parabolic dish concentrators as oven to produce thin films.

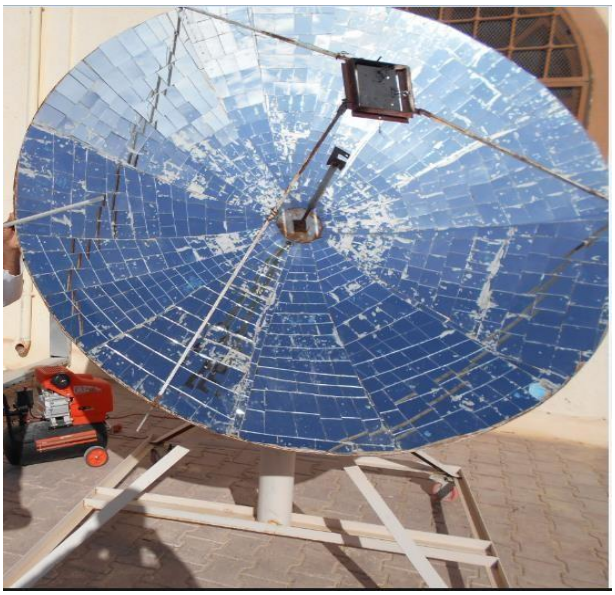

Figure I. 4: General view of the solar concentrator used (laboratory22, Echahid Hamma Lakhdar University, El Oued). [62].

- **Thin Film Production**

One of the most recent applications of solar energy is the production of thin films, in which the reflecting dish is used to produce heat by focusing sunlight on a glass plate and spraying the solution to be applied on the surface. In this case, the electric heater is replaced with a more ecologically friendly alternative.

I.3. Thin films

I.3.1. Definition of Thin Film

In theory, a thin layer of a given material is an element of that material, one of whose dimensions, called thickness, has been greatly reduced to the point where it can be expressed in nanometers, and this low distance between the two boundary surfaces (this quasi two-dimensionality) causes a disruption of the majority of the physical properties [11]. The fundamental distinction between a material in the solid state and a material in thin layers is that in the solid state, the function of the limits in the characteristics is often overlooked, but in a thin layer, it is the effects related to boundary surfaces that predominate [12]. The effect of two-dimensionality will be increased when the thickness of a thin layer decreases, and when the thickness of a thin layer passes a particular threshold, the influence of thickness will become minor and the material will regain its characteristics. a well-known solid substance [13] **(Figure I.5)**.

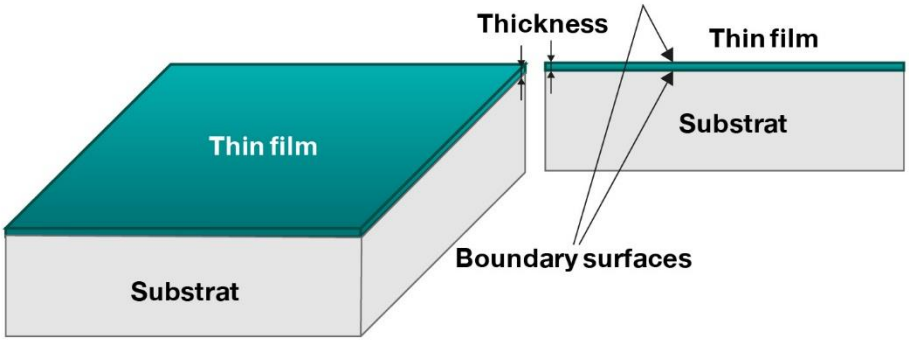

Figure I. 5: Schematic of thin film deposited on a glass substrate.

The second important quality of a thin film is that it is always integrated with the support on which it is created, regardless of the manufacturing process utilized. As a result, it will be critical to factor in this important element in the design, namely that the support has a significant impact on the structural characteristics of the layer deposited on it. Thus, depending on whether it is placed on an amorphous insulating substrate such as glass or a monocrystalline silicon substrate, a thin layer of the same material with the same thickness may have very different physical characteristics.

The following conclusion derives from these two key features of a thin film: a thin film is anisotropic in construction.

Preparing thin films may be done in a variety of ways [14]. We will only mention the most often used in the field of electronics, which would likely to omit practically all particular chemical, pharmacy, and biology applications and procedures.

Physical processes for depositing material on a substrate that is originally devoid of deposit are the most common production methodology utilized by producers of active and passive electronic components. As a result, the thin layer's thickness will increase from zero [15,16]. Although there are pickling procedures that allow you to level a material angstrom by angstrom, this method is almost never utilized to obtain a thin coating of a specific thickness.

In practice, there are two main families of methods: those that use a carrier gas to move the material to be deposited from a container to the substrate and are similar to diffusion techniques used in the manufacture of active components, and those which involve an environment at very reduced pressure and in which the material to be deposited will be conveyed thanks to an initial impulse of thermal or mechanical nature [17].

I.3.2. Applications of Thin Film

Thin film manufacturing technology has found applications in a wide range of industrial sectors, most notably electronic components, sensors, optics, and protective surfaces **(Figure I.6)**.

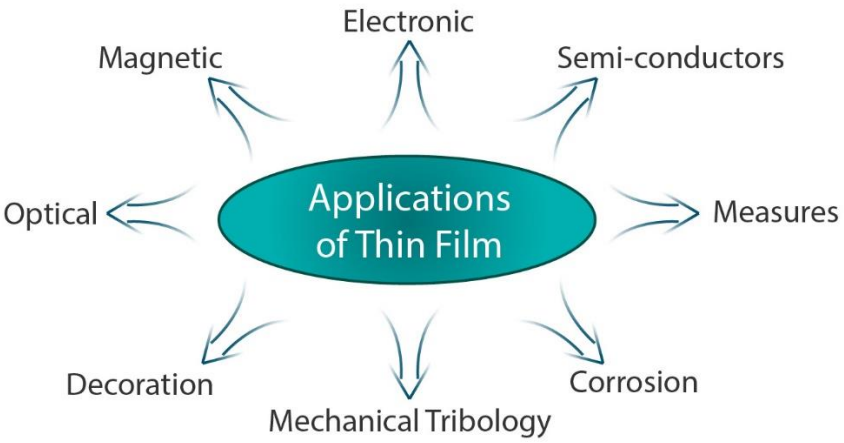

Figure I. 6: Applications of thin films [11].

Thin films will be employed in electronics for interconnections between various devices distant from a chip, for example. We will utilize thin layers of aluminum, gold, or copper for this, as these are good conductors and reasonably inexpensive. Thin films can also be utilized in hard disk read heads. Then, magnetic thin films are utilized. The thin layers will be employed in optics to create anti-reflection films, glasses, automotive windshields, and even reflective films. Similarly, thin layers can be utilized to create anti-corrosion surfaces, surfaces that allow the materials on which they are placed to harden, or even decorative surfaces.

I.3.3. NiO thin films

I.3.3.1. Definition of Nickel oxide (NiO)

Bunsenite, or nickel oxide, is a basic oxide. Depending on the manner of preparation, it takes the shape of a greenish gray powder. It is both a transition and an antiferromagnetic substance [18]. Their Néel temperature is 523 K, which is the temperature that antiferromagnetic materials are defined by. Sub-lattice atoms naturally magnetise in the form of a ferromagnetic lattice in lower temperature, and the curie temperature is approximately 2000 K [19].

Figure I. 7: Hydrated nickel chloride.

The antiferromagnetic order of nickel oxide is linked to the crystal's symmetry characteristics (body-centered cubic structure, face-centered cubic, perovskite). It exhibits high chemical and thermodynamic consistency [20], as well as a strong resistance to oxidation [21]. Some of the general characteristics of NiO are described in Table 1.1. NiO is quite scarce in its raw, natural form. As a consequence, it is necessary to synthesise it. NiO can be synthesised by a variety of methods. Pyrolysis of Ni2+ compounds such as hydroxide, nitrate, and carbonate, which produces a light green powder, is the most frequent technique. The production of black NiO powder when heated in an oxygen or air environment indicates nonstoichiometry.

Because of the presence of Ni3+ due to Ni vacancies, nonstoichiometry is accompanied by a color change from green to black [22].

I.3.3.2. Properties of hydrated nickel chloride

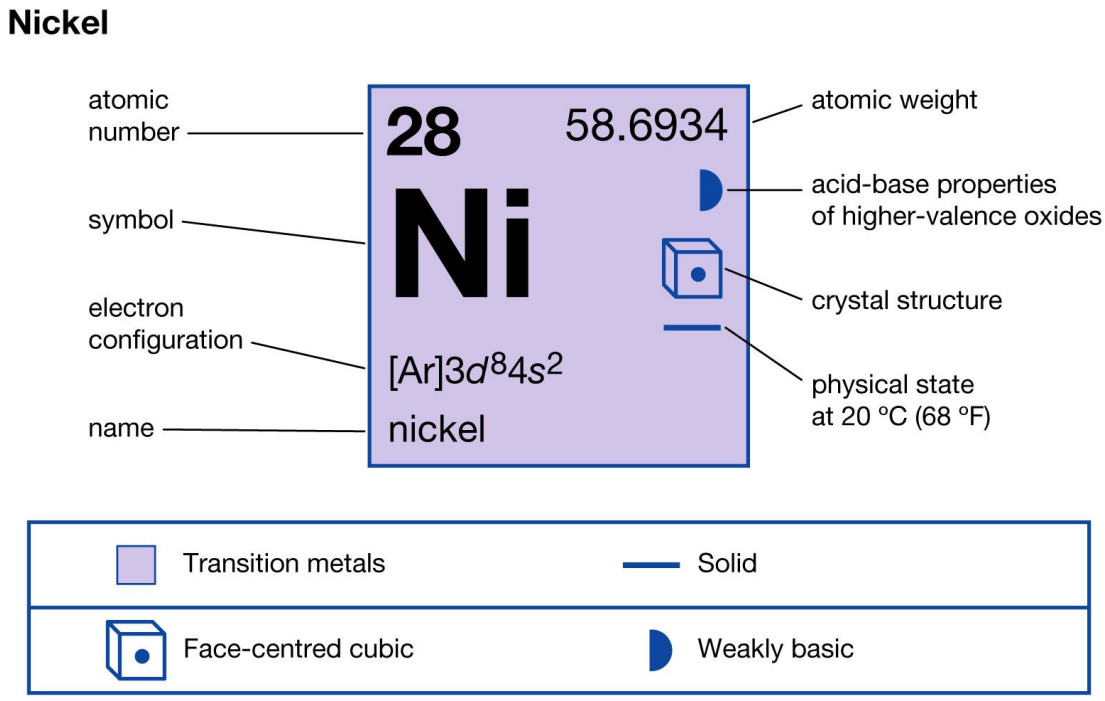

Figure I. 8: Properties of Nickel (Ni) element [23].

Table I. 2: The table shows element percentages for NiO (nickel oxide) [24].

Element	%
Ni	78,58
O	21,42

NiO is an appealing p-type transparent semiconductor that is being investigated for a wide range of applications. We present a thorough investigation of the electrical characteristics of NiO produced by atomic layer deposition that are relevant to hole-transporting materials in solar energy conversion applications (ALD). [25]

Table I. 3: General properties of NiO.

Average atomic number	18
Average atomic mass **(g)**	27.35
Molar mass **(g / mol)**	74.69
Boiling point **(° C)**	>2000
Solubility in water **(mg / L)**	1.1 at 20 ° C. insoluble
Melting point **(° C)**	1990 – 1960
Enthalpy of formation at 298k	-240 KJ / mole of atoms
Entropy S_0 **(JK-1.mol-1)**	38.00

I.3.3.3. Crystallographic and Structural Properties

Figure 1.19 shows nickel oxide (NiO) crystallisation in a NaCl framework (rock salts). A face-centered cubic structure (FCC) is used to construct it [26, 27]. Because this cubic structure is made up of two similar subnetworks A and B, each atom in subnet A has only subnet B neighbours and vice versa. A CFC structure exists in the anionic (O2-) and cationic (Ni2+) subnetworks. The plane (100) is a mixed-metal plane that contains 50% nickel and 50% oxygen. Pure Ni and pure O alternate in the planes (111). The polar (non-stable) face (111) is different from the non-polar (stable) face (100) [28]. The interplanar spacing between two different planes is 0.120 nm, almost double the distance between two equivalent planes. The major crystallographic characteristics of this oxide are summarised in Table 1.2.

Crystalline solids have a periodic structure in their crystal structure. Although perfect stoichiometric metal oxides are insulators, the electrical, optical, and mechanical characteristics of the crystal change when different flaws are introduced. It should be noted that the presence of flaws is dependent on the method of growth and the material development conditions.

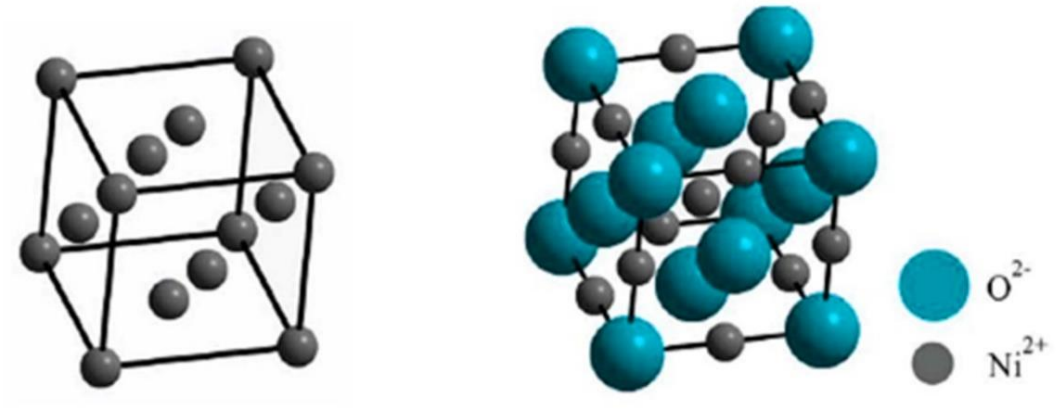

Figure I. 9: Crystallographic structure (a) of nickel (b) nickel oxide [28].

I.3.3.4. Electronic and electrical properties

The band structures of transition metal oxides determine whether the oxide is insulating or semiconductor, depending on the values of the prohibited bands. Nickel oxide is a transition metal that belongs to an important family due to its applications. Their magnetic behavior is owing to the presence of an energy band known as "band d." The 3D wave functions are confined to the area of the atomic nucleus. The band d can hold up to ten electrons and has a width of about 5eV [29]. In the 3D electronic sub-layer, the total energy accountable for magnetism was somewhat greater than in the 4s conduction sub-layer. The orbitals of the oxide ions in recovery and the 3D orbitals of nickel form the low energy linker level, which is composed of two levels, t2g and eg (Figure I.10). This level and the t2g level are electrically whole, whereas the antibonding eg level only contains two electrons. The electrical combinations of nickel and oxygen are as shown: O: (He) 2s2 2p4 [28]. Ni: (Ar) 3d8 4s2, O: (He) 2s2 2p4 [28].

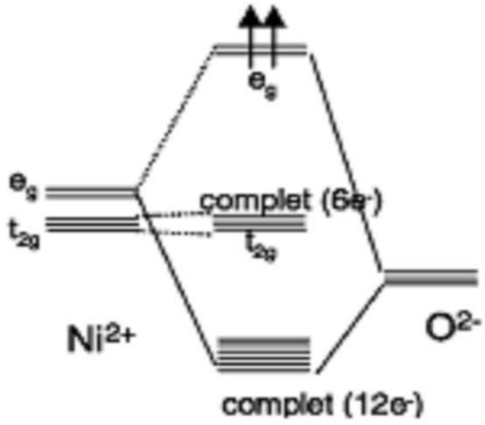

Figure I. 10: Schematic diagram of NiO energy levels.

Pure, stoichiometric NiO is a fantastic insulator. NiO's conduction mechanism has yet to be fully explained, hence there is no universal agreement on its electrical properties [30]. In the beginning, stoichiometric NiO was believed to be a Mott insulator [31]. It's then rectified into a Mott-Hubbard type insulator [32], however after getting oxidised, it turns into a p-type conductor [33]. The conflicting findings, on the other hand, demonstrate the complexity of NiO's conduction mechanism and electronic structure [34].

Table I. 4: Some electrical properties of NiO [35].

Conductivity σ $(\boldsymbol{\Omega.Cm})^{-1}$	≤ 0.1
Mobility $\boldsymbol{\mu}$ $(\boldsymbol{cm^2/V.S})$	0.1^{-1}
Electronic densities $\boldsymbol{N}$ $(\boldsymbol{cm^3})$	$10^{18} - 10^{19}$
Prohibited band energy $\boldsymbol{Eg}$ $(\boldsymbol{eV})$	$3.5ev - 4ev$
Dielectric constant	11.9

I.3.3.5. Optical Properties

Because of significant absorption in violet (2.75 – 2.95 eV) and red 1.75 eV in transparent conductive oxides (TCO), which have high conductivity and lighting gap energy directly, nickel oxide is green. The high absorption coefficient of the green area (1.75 – 2.75 eV) increases in the availability of free oxygen, particularly when Ni is oxidised by straight oxygen or doping with Li+ [34]. Based on the deposition method, the band gap of NiO thin films ranges between 3.6 and 4 eV. To better understand the electrical structure of NiO, several optical investigations, such as photoemission or inverse photoemission studies, have been carried out [29]. Theoretical computations on optical spectra have also been reported. It's worth noting a few key features of NiO's conduction band, valence band, and optical band gap:

1. Ni 3d states dominate the conspicuous structure at the valence band edge [36].

2. Ni 4s is identified at the apparent structure of the conduction band edge [37], however the construction on the small shoulder ((Ec-E) 0.8 eV) is identified and regarded as localised Ni states.

3. The band structure's gap is clean due to its nature; however, the mid-gap structure is extremely vulnerable to thin film deposition and imperfections [37].

I.3.4. Methods of Thin-Film Deposition

Due to its remarkable technological importance and scientific interest in their characteristics, many materials have been produced in the form of thin films throughout the years. They can be used for anything from nanostructures to multi-square-meter window glass coatings. Based on the nature of the deposition process, thin film deposition methods are classified into two categories: physical and chemical deposition methods. One of the physical processes (PVD), along with laser ablation [39], molecular beam epitaxy [40], and magnetron sputtering [41, 42], is physical vapour deposition. Chemical deposition techniques include gas phase and liquid phase deposition (Figure I.12). Chemical vapour deposition (CVD) and atomic layer epitaxy (ALE) [43] are gas phase techniques, whereas spray pyrolysis [44, 45], and sol-gel [46], electrodeposition [47], chemical bath deposition (CBD) [48], liquid phase epitaxy (LPE) [49], spin- coating [50] and dip-coating [51] are liquid phase methods .

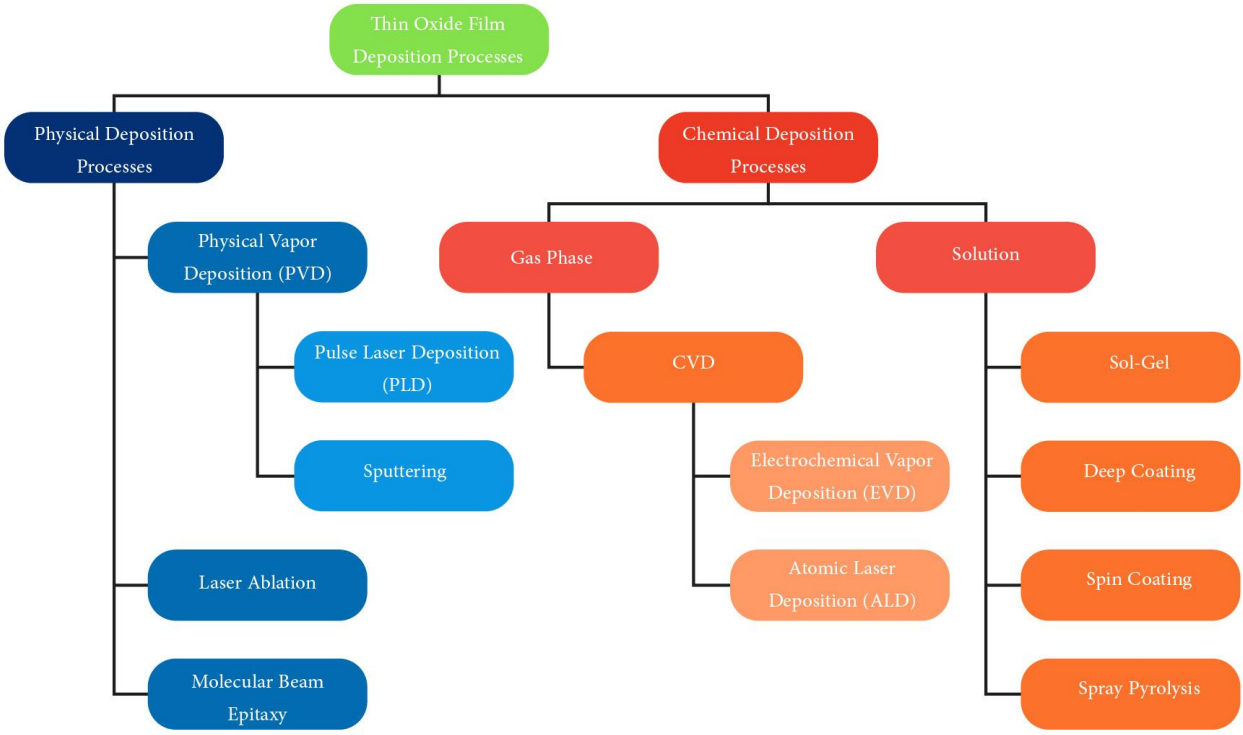

Figure I. 11: Schematic diagram of thin film deposition [52].

I.3.4.1. Physical Vapor Deposition (PVD)

PVD techniques **(Figure II.11)** are deposition procedures in which atoms or molecules of a material are vaporized from a solid or liquid source, transferred as a vapor via a vacuum or low-pressure gaseous environment, and condense on a substrate. PVD methods can deposit films made of elemental, alloy, and compound materials, as well as some polymeric materials.

PVD processes are classified as follows:

Material from a thermal vaporization source reaches the substrate without colliding with gas molecules in the space between the source and the substrate in vacuum evaporation. Sputter deposition—a surface (target) exposed to physical sputtering is the source of evaporated material. Sputter deposition should be further classified into high- and low-pressure sputter deposition based on film characteristics. Arc" vapor deposition—uses a high current, low voltage electric arc in a low pressure gas to erode the solid cathodic electrode or melt and evaporate the anodic electrode.

Plating of Ion is a method that entails changing and regulating the composition and characteristics of a depositing layer by blasting it with atomic-sized energetic particles on a continuous or periodic basis. In ion plating, vacuum evaporation sputtering or arc vaporisation can be utilised as a substrate of depositing material. Ion beam assisted deposition (IBAD) fusillades the depositing layer with stable or reactive ions to alter its properties and, in the case of a reactive ion, to stimulate chemical reactions. The different PVD procedures are described in **(Figure II.11).**

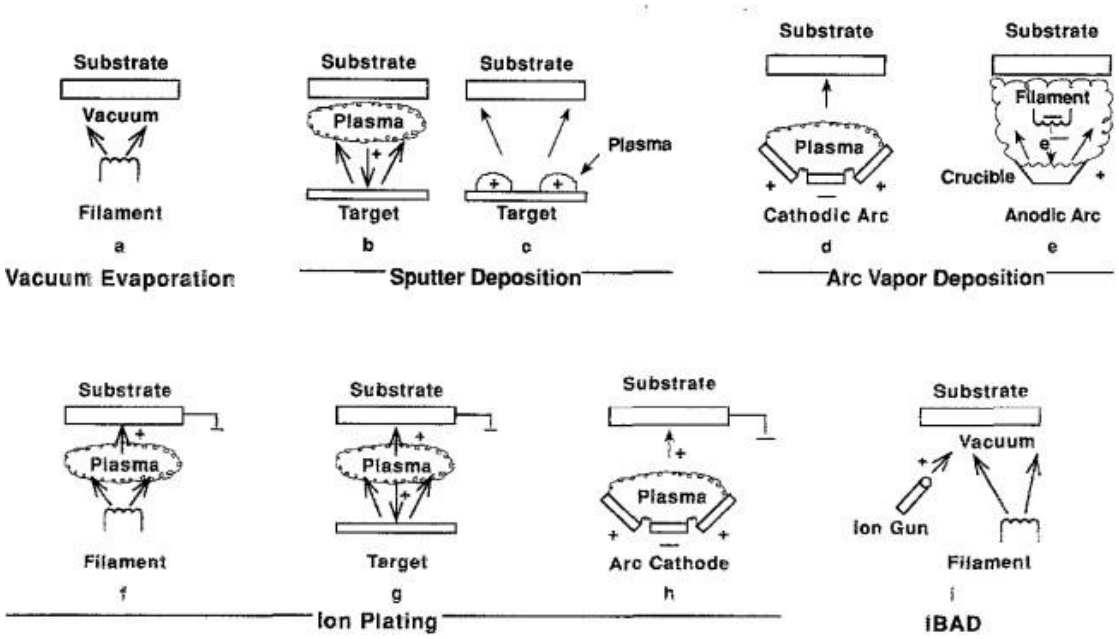

Figure I. 12: Schematic views PVD processing technique [53].

I.3.4.2. Chemical Vapor Deposition (CVD)

I.3.4.2.1. An Overview of Chemical Vapour Deposition

Since its inception as an efficient way of creating a broad variety of elements and products with potentially changeable material compositions, chemical vapour deposition (CVD) has

been established as an innovative manufacturing technology in a wide range of industrial sectors. Namely, the latter include the semiconductor and ceramic productions. As a consequence of intensive research and development efforts by academic researchers and industrial end-users, the tendency of extending its applications from initial mass semiconductor and microelectronics manufacturing to a wider range of applications has gained considerable importance. [54]

I.3.4.2.2. Definition of CVD

The deposition of a solid on a heated surface as a consequence of a vapor-phase chemical reaction is known as chemical vapour deposition. It is an atomistic vapor-transfer technique, which implies the deposition species are atoms, molecules, or a combination of the two. Apart from CVD, they also include PVD techniques such as evaporation, sputtering, molecular beam epitaxy, and ion plating [54]. Chemical Vapor Deposition (CVD) has emerged as a critical tool in the semiconductor industry. The Boundary Layer Theory (BLT), which describes how the CVD response occurs, is essential for comprehending the CVD mechanism. A process engineer with a broad knowledge of BLT may make smart changes to a complex process. Understanding BLT is essential for semiconductor engineers when researching new CVD methods such as epitaxial, mid-temperature, low-temperature, and plasma-enhanced deposition. [56]

Chemical vapor deposition (CVD), in its various forms, is a vital thin-film deposition process. The elements of the film to be deposited are delivered into a reaction chamber as a vapor or gas in traditional CVD. In many cases, the precursors are liquids or solids that must be heated at low pressure in order to contribute enough vapor to create reasonable deposition rates. Certain precursors are unstable and breakdown under these settings in some circumstances. Many of these CVD precursors are costly. Deposition of multielement coatings typically necessitates the use of a complicated system to handle the numerous elemental precursors. [57]

(Figure I.14): illustrates a detailed CVD system in which reactant gases, often known as precursor gases of CH_3SiCl_3 and H_2, are injected at a preset temperature into a reaction chamber. As the gases pass through the reactor, they make contact with a heated surface, where they react and form a solid SiC layer on the surface of the substrate. In most cases, an inert gas, such as Ar, is used as a diluent gas. The depositing temperature and pressure are critical factors in this process. Following the reactions, the HCl-containing exhaust gases are collected by NaOH before being condensed by a liquid N_2 trap and discharged into the atmosphere.

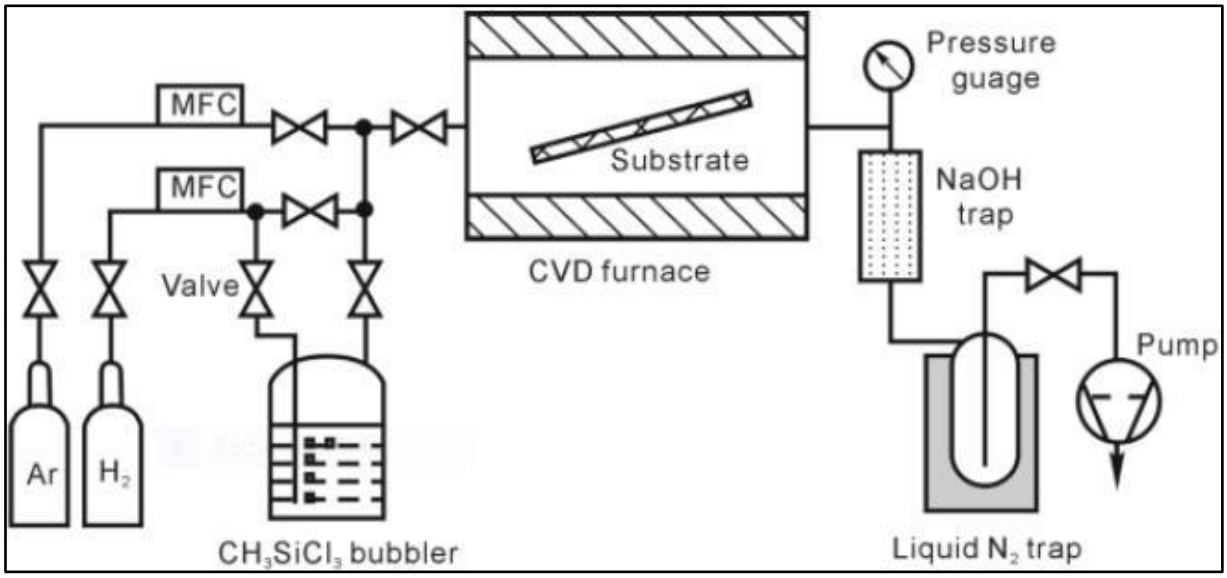

Figure I. 13: Schematics of a CVD process: arrangement of a CVD system.

CVD is thus a catch-all term for a series of techniques that involve the formation of a thin layer by chemical reaction and the deposition of a solid material layer onto substrates.

(Figure I.14) Spear [58] presents a model that includes the sequential physical and chemical phases that occur during a CVD process.The latter are as follows:

1. Mass transport of reactant gaseous species to the vicinity of the substrate.
2. Reactant species diffusion to the substrate surface through the boundary layer or homogenous chemical reactions to produce intermediates.
3. Adsorption of reactant species or intermediates on the substrate's surface
4. Surface migration is exemplified by heterogeneous reaction, integration of coating atoms into the growing surface, and the generation of by-product species.
5. Desorption of surface reaction by-product species
6. By-product species diffusion into bulk gas
7. Substrate removal of by-product gaseous species (exhaust).

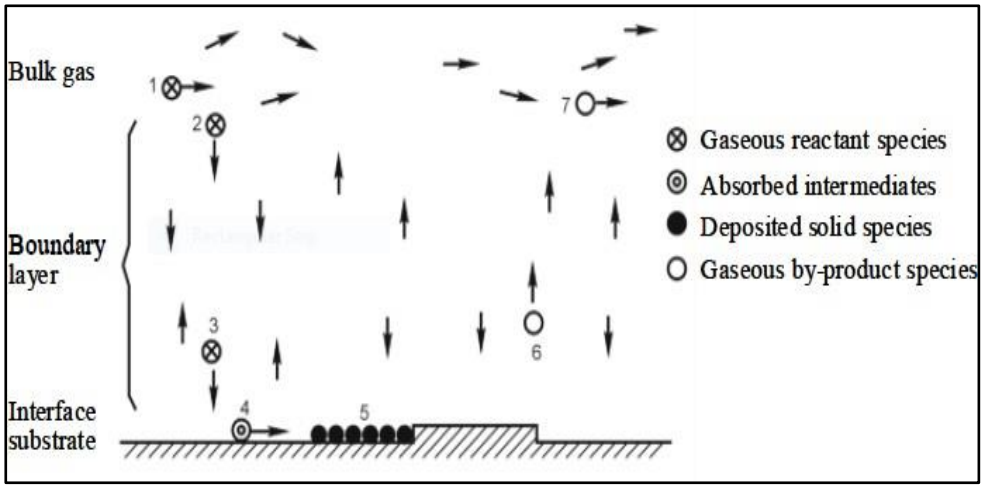

Figure I. 14: Schematics of a CVD process: a CVD model.

I.3.4.3. Spray Pyrolysis Technique (SPT)

I.3.4.3.1. Principle

Spray pyrolysis is a processing technique researched for the production of thin and thick films, ceramic coatings, and powders. In comparison to several other film deposition methods, spray pyrolysis is a very straightforward and cost-effective processing technique (especially in consideration of equipment costs). It offers a very simple technique for creating films of any composition. Spray pyrolysis does not require the use of expensive substrates or chemicals. The technique has been applied to dense film deposition, porous film deposition, and powder production. Even layered films may be easily produced using this flexible technique.

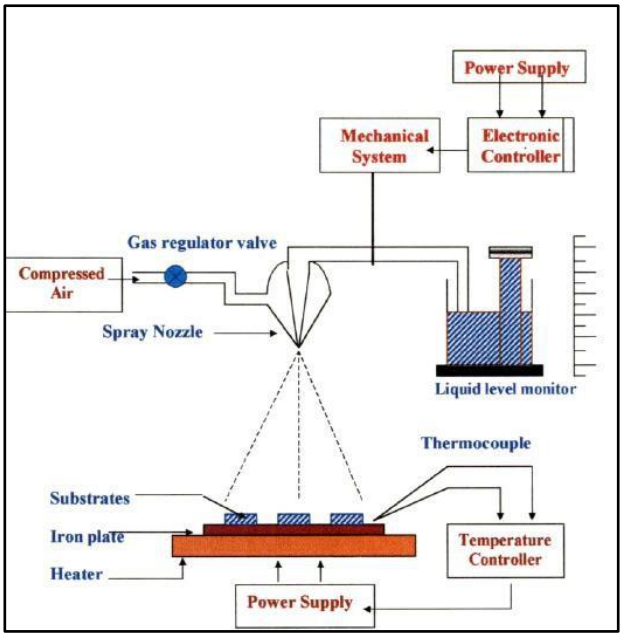

Figure I. 15: Schematic diagram of Spray pyrolysis system [59].

Spray pyrolysis equipment typically includes an atomizer, precursor solution, substrate heater, and temperature controller. Air blast (the liquid is exposed to a jet of air), ultrasonic (ultrasonic frequencies produce the short wavelengths needed for precise atomization), and electrostatic atomizers are frequently employed in spray pyrolysis (the liquid is exposed to a high electric field). [60]

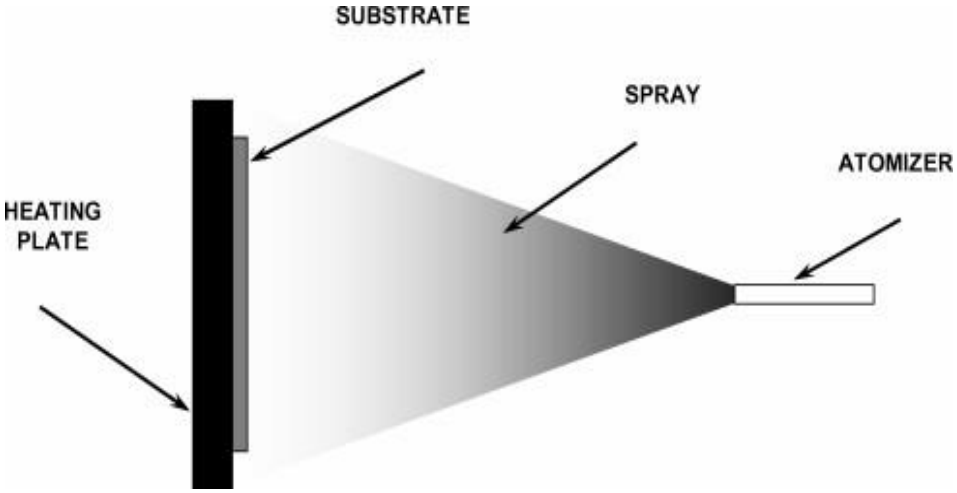

Figure I. 16: Schematic diagram of spray pyrolysis equipment.

I.3.4.3.2. Diagram of Pyrolysis and Thin-film Deposition

Spray pyrolysis experimental factors such as precursor solution, precursor breakdown, atomization, and aerosol transport are critical in evaluating the structural, compositional, surface topological, electrical, and optical characteristics of thin films. Several of these requirements are addressed in the next section.

I.3.4.3. Factors influencing thin-film creation using the spray pyrolysis method

Two variables that affect the film formation process are the automation of the spray solution into a spray of tiny droplets with regard to the spraying nozzle geometry and the pressure of a carrier gas.

Substrate temperature, solvent evaporation, droplet size, carrier gas, spray rate in the ambient environment, and cooling time after deposition all have a significant impact on the characteristics of produced films.

The film thickness, on the other hand, is proportional to the solution concentration, the distance between the substrate and the nozzle, and the substrate temperature [61].

I.3.4.4. Merit of Spray Pyrolysis Technique

It provides a straightforward method for depositing films with virtually any component in any proportion by simply adding it in some form to the spray resolution.

When compared to the closed CVD approach, the spray pyrolysis approach does not require prime grade targets and/or substrates, nor does it require a vacuum at any point, which is a significant advantage if the approach is to be used for industrial applications.

The thickness of the films and the deposition rate may be easily regulated using spray settings, eliminating the fundamental disadvantage of chemical methods such as sol-gel, which generate films of limited thickness.

- This method operates at averaged temperatures ranged in 200-600 degree Celsius.
- It doesn't cause native heating that may be damaging the materials to be deposited.
- Practically there are no limitations on the substrate material, dimension or its surface profile [61].

I.3.4.5. Deferent Type of Spray Pyrolysis Devices

Spray pyrolysis technology is one of the best and easiest methods. In addition, the device used for spray pyrolysis method has two types: electronic oven, which is the device used all over the world, and solar oven [62].

- **Solar oven**

It is a new method that differs from the classic method in the heating part. We heat the substrate holder by focusing the sun's rays on the holder in order to obtain the temperature required in the experiment. Whereas the PDC is used as a furnace instead of an electronic furnace.

The solar oven is made up of the following elements **(Figure .I.18):**

- Reflector
- Receiver
- Support
- The tracking system
- The mirror

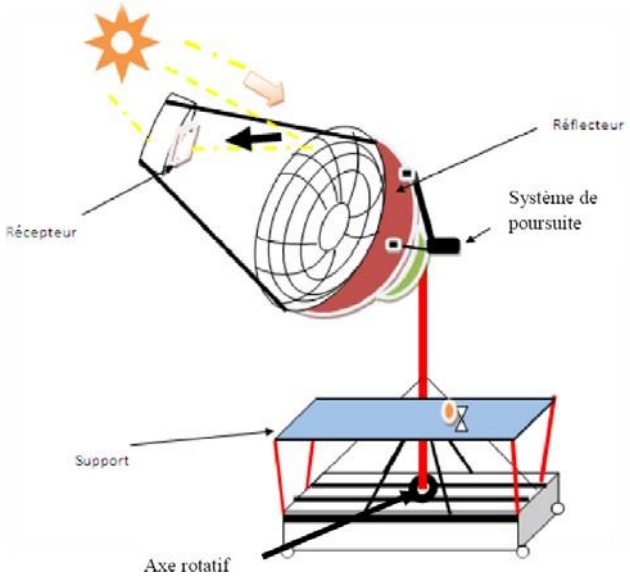

Figure I. 17: Complete assembly of the solar oven [62].

II.7 Conclusion

In this chapter, we began learning about the structure and characteristics of the sun, then the energy that we can get form it. In addition, we talked about solar field in Algeria and application of solar energy. After that, the description of a solar collector dish as an oven to produce thin films.

Second, we have presented the different structural, electronic, electrical and optical properties of NiO thin films. As well, we talked about thin film deposition methods we discussed the principle of spray pyrolysis solar deposition. In the next chapter we are going to see more details about spray pyrolysis solar deposition and the Techniques for Elaboration and characterization devices for (NiO) thin films

Chapter II
Techniques for Elaboration and characterization devices for (NiO) thin films

Chapter II: Techniques for Elaboration and characterization devices for (NiO) thin films

II.1. Introduction:

In this chapter; we introduce the experimental details of NiO deposition, including the description of the equipment and deposition procedures used. Then the preparation of the substrate and precursor solutions are described. And different characterization techniques (1.DRX, 2. Four-point technology, 3. UV-visible spectroscopy) used to analyze and determine the different structure, optical and electrical properties of NiO thin layers.

II.2. Elaboration Techniques of (NiO) thin films:

II.2.1. Experimental Montage used:

It is a frame produced in the mechanical engineering laboratory 22 of El Oued University. It is made of simple elements. We have modified this to produce Nickel (NiO) thin film in a new way.

The solar concentrator consists of the following elements:

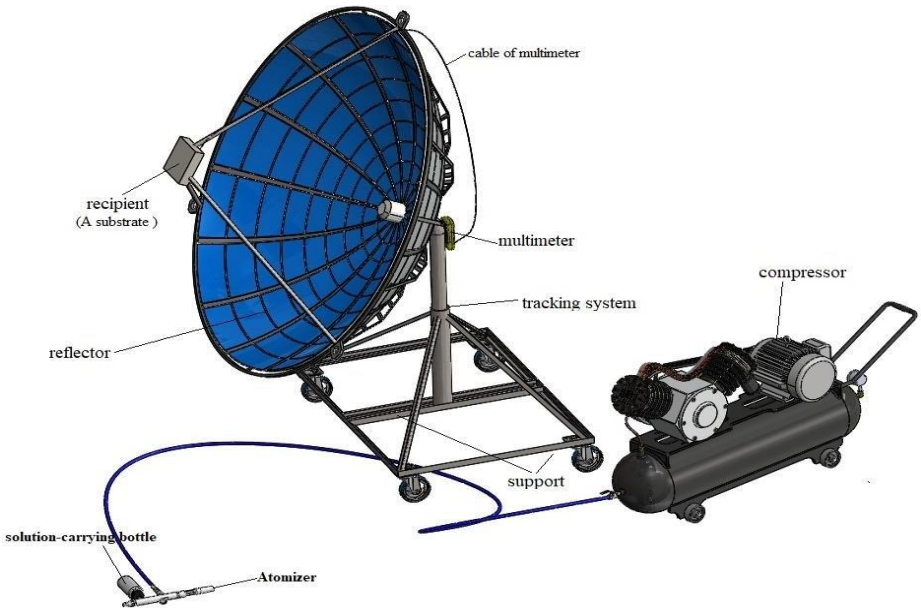

Figure II. 11: Complete assembly of the solar oven used (Designed by Solidworks) [63].

- **Reflector**

A paraboloid of revolution is the surface produced by rotating a parabolic curve around its axis. Solar concentrators with a reflecting surface are also known as parabolic concentrators.

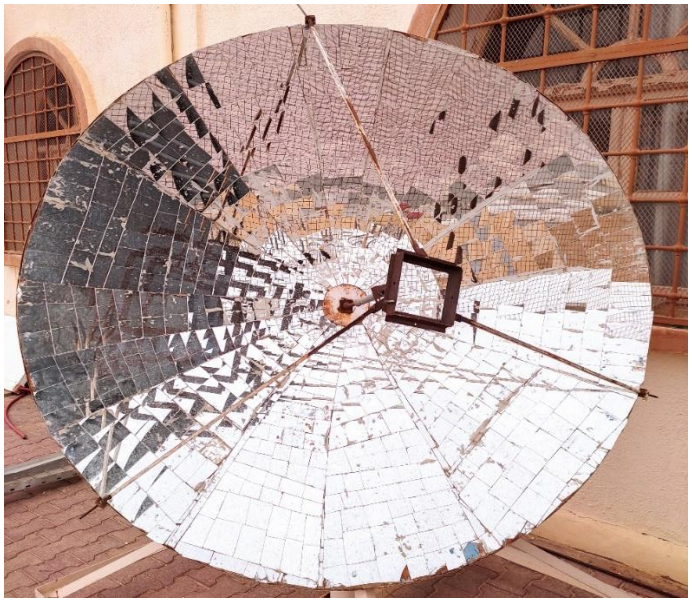

Figure II. 2: General view of the reflector used.

The reflector made up of several mirrors which cover the interior surface of the reflector .As shown in (figure .II.2). Mirrors should have their shiny sides facing the sun. The parabola rests on a mobile support which facilitates its movement in addition to the tracking mechanism operating using two axes.

- **Receiver**

The solar receiver converts concentrated solar radiation into usable heat. The receiver is the hottest component in the solar cooker system. The efficiency of the solar receiver reflects its ability to transfer the maximum amount of radiative power incident to the heating plate at working temperature with minimal thermal losses. The active element of the receiver is the hotplate [64].

The surface of the receiver must have the following characteristics [65]:

- Good conductivity and thermal diffusion

- An absorption factor as close as possible to unity.

Heating plate: this is a plate placed in the focal zone of the dish facing the reflector.

Table II. 1: Geometric characteristics of the receiver.

Length	L =0.15 m
Depth	h =0.02 m

Figure II. 3: shows a real image of the receiver used.

- **Support**

It is an element that holds the above components together and allows the oven to rotate to follow the sun as it moves in the sky and allowing its panel to be installed in the most favorable location. . As shown in figure II.4

Figure II. 4: Photo of the metal support.

- **Tracking system**

It is a system that follows the course of the sun from multiple angles, so that it completely irradiates the panel. This improves the efficiency of solar panels by 30 to 40%.

Our system adopted a very simple tracking mechanism based on a (jacks and a rotary axis) to turn the solar oven to the position of the sun at any time. As shown in (figure .II.5).

Figure II. 5: Photo of the tracking system containing a cylinder and a rotary axis.

- **Atomizer**

It is an element that turns the solution into droplets. It is placed on an adjustable height support in order to control the beak-substrate distance.

- **Compressor**

It is a device that supplies the pressure to the atomizer in order to operate it. As shown in figure II.6

Figure II. 6: The compressor increases the required pressure.

II.2.2. selecting and preparing of the substrate:

The quality of the deposits and the quality of the samples depend on the cleanliness and condition of the substrate. Therefore, cleaning is a very important step. All traces of grease and dust should be removed, and the surface of the substrate should be visually inspected for scratches or unevenness. These conditions are essential for the good adhesion of the deposit to the substrate and its uniformity (constant thickness).

We use (CITOPLUS-REF-0302-0004) type glass substrate. . As shown in (**Figure II.7)**

These substrates have been cleaned to ensure the adhesion of the layer. This cleaning process is divided into the following stages:

- Wash in an acid bath for 5 min.
- Wash with distilled water, then with acetone for 15 min.
- Wash with distilled water.
- Drying the glass substrates.

Figure II. 7: The type of substrate used.

II.2.3. Selecting material:

In this part, we give some physical and chemical properties of nickel(II) nitrate hexahydrate . As shown in **Table II.2**:

Table II. 2: Some physical and chemical properties of nickel dinitratehexahydrate [66]

Appearance	Solid green color
Odour	scentless
The molecular formula	$Ni(NO_3)_2$ .6H2O
Molecular molar mass	290.79 g/mol
Density	2.05 g/cm3
Fusion point	56.70 ° C
Boiling point	136.70 ° C
Solubility	Soluble in water and in methanate

Nickel dinitratehexahydrate is prepared by the reaction of nickel oxide with nitric acid: $NiO + 2\ HNO3 + 5\ H2O \rightarrow Ni\ (NO3)2.6H2O$

II.2.4. Adjustable parameters:

In order to obtain reproducible thin films with good adhesion, it is necessary to start studying various parameters that directly affect the thin films deposition. The development of various deposition parameters requires some tests.

In order to obtain a reproducible thin layer with good adhesion, it is necessary to start studying the various parameters that directly affect the deposition of the thin layer. The development of various repository parameters requires some testing.

Spraying is a deposition process and depends on various conditions, such as:

- Substrate temperature.

And in this experiment, we study the substrate at five different temperatures

II.2.5. Measuring instruments:

II.2.5.1. Measuring temperature:

We used a digital multimeter (ALTAY) with the following characteristics:

- Model IEC61010-1
- Operating range: 0 - 1000°C.
- Power supply, single battery (9V).

Figure II. 8: digital multimeter (ALTAY).

II.2.5.2. Measuring pressure:

Also, we used a pressure measure with the following characteristics:

- Model DAC 24D
- Operating range: 0 – 12 bar.

Figure II. 9: pressure measure.

II.2.5.3. Measuring Wind speed

We used a digital Thermo-Anemometer (AMPROBE) with the following characteristics:

- Model: TMA5
- Wind speed range: 0.5 – 44.7 MPH.
- Air Temperature range: 0 – 50°C.

Figure II. 10: digital Thermo-Anemometer

II.2.5.4. Measuring Mass:

We used a digital scale (MIHEE) with the following characteristics:

- Model: MH-999
- Capacity: 600g × 0.01g.
- Operating temperature range: 10 – 30°C.

Figure II. 11: digital scale

II.2.6. Experimental conditions:

- Solution volume: 5 ml. (5 samples)
- Solution concentration: 0.1 mole l^{-1}
- Substrate temperature: (350, 375, 400, 425 and 450°C). As shown in (Figure II.12)
- The distance between the spout and the substrate: 10 cm.
- Pressure: 2 bar. . As shown in figure II.9

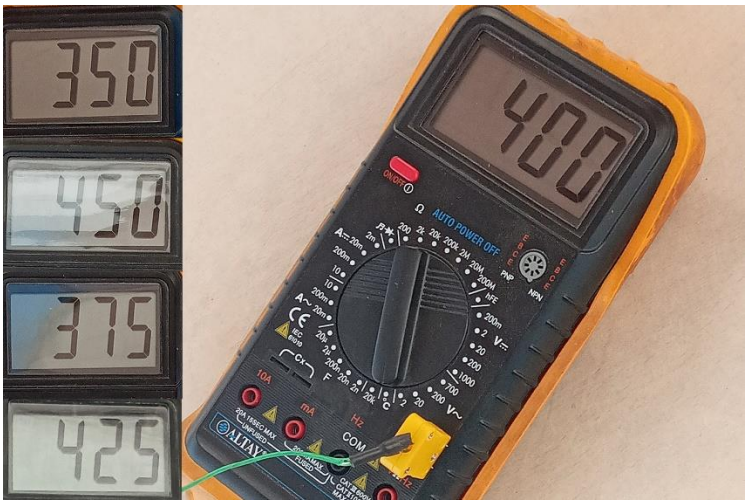

Figure II. 12: The temperature at which the substrate is heated (350-450 C°).

Figure II. 13: Sensitive electrical balance MH-999.

The solution was prepared according to the relations:

$$n = C \times V \qquad \text{(II.1)}$$

$$n = \frac{m}{M}$$

$$m = M \times C \times V \qquad \text{(II.3)}$$

n:$materialquantity$

m:$Mass$

M: $Molarmass$

C: $concentration$

V: $volume$

II.2.7. Steps of the experiment:

In this experiment, we made thin layers with NiO deposited using solar concentrators, where the process took place in several stages:

- **Prepare the solution:**

We prepare 2.98 g of nickel dinitratehexahydrate Ni (NO3)2 6H2O and put it in a beecher containing 100 ml of distilled water and mix them using a magnetic mixer for 30 minutes at a temperature of 20 ° C.

Figure II. 14: Nickel dinitratehexahydrate [66]

- **Setting the oven:**

The ideal operation of the oven is when the solar radiation is parallel to its axis of the substrate holder, we have period when our device is in a clear sky environment.

The oven faces the sun. Use a controlled tracking system. Since the sun rose, it has been redirected to the position of the sun. The sun's rays are reflected at the focal point of the parabola to form a black spot, which should appear on the front of the plate to be heated. As shown in figure II.15

Figure II. 15: Setting the oven manually

- **Multimeter location**

To measure the temperature reached on the surface of the oven, we placed the multimeter probe on the surface of the receiver.

Figure II. 16: Temperature measuring device and the detector

- **Prepare the substrate**

The process is done by washing the substrate in an ethanol solution and then in distilled water to remove any organic traces that may affect the results of the experiment.

- **spraying process**

We take 5 ml of the solution using a measuring needle and pour it into the solution holder and then spray it on the substrate at a specified temperature (350 – 450 °C).

II.2.8. Problems encountered:

The problems encountered in the production process of the thin films using parabolic concentrator prototype, can be summarized as follows:

- The problem of reading temperature, because its value will change rapidly under the influence of wind speed.
- The problem of fixing the multimeter probe and spray system (atomizer) in front of the glass substrate holder.
- The problem that the solution is evenly sprayed on the substrate.

II.3. Characterization techniques

In the following paragraphs we have explained the different techniques used for characterize and measure structural, electrical and optical properties.

II.3.1. Structural Characterization - X-ray Diffraction (DRX)

Diffraction of X-rays powder sample crystallography is well-established and extensively utilised. Material characterisation is the study of the atomic structure of different substances in different states. Of course, significant progress has been achieved in this field. Max von Laue since 1912, followed in 1913 by W.L. Prague and W.H. Prague. The study of the appearance of natural minerals is the foundation of crystallography, and a significant quantity of data has been systematised via the use of geometry and group theory. Then, crystallography became a useful technique for considering how to build crystals from tiny units, which corresponded to the endless repeating of the same structural unit in space. [67]

II.3.1.1. Principle of DRX analysis

When a monochromatic X-ray beam is directed at a poly-crystalline material, itis partly reflected by the atomic planes of some crystals. **Figure II.17**

The diffraction will occur only in crystallized materials and when the Bragg relationship is verified:

$$2d_{hkl}\sin\theta = n\lambda \quad \text{(II.4)}$$

d_{hkl}: is the inter-reticular distance, that is the distance between two crystalline-graphic planes,

θ: the angle of incidence and therefore the angle of reflection in relation to these planes,

λ: the wavelength of photons X incidents,

n: the diffraction order (integer).

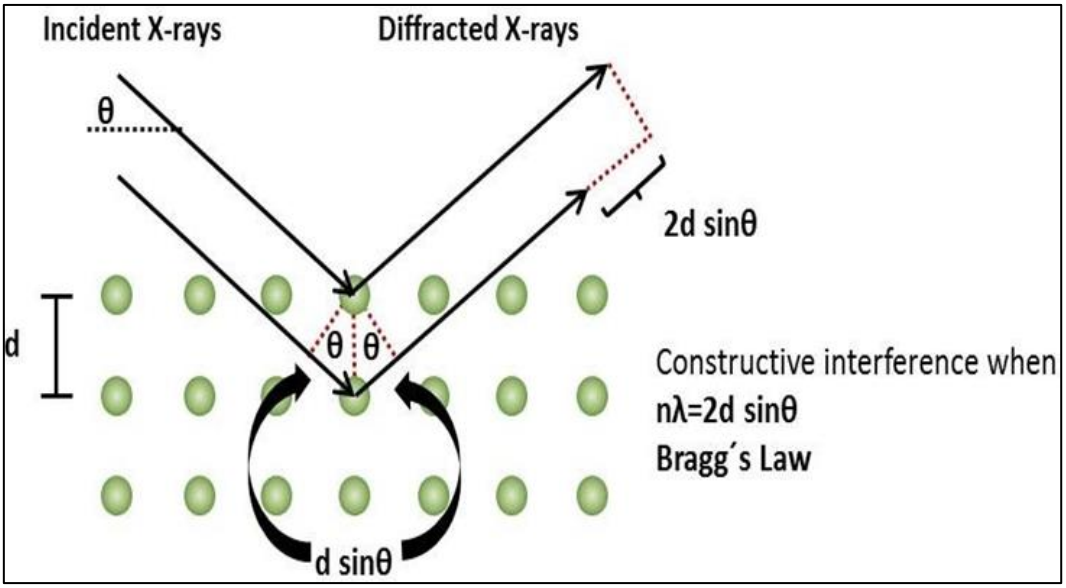

Figure II. 17: Schematic diagram of the Bragg equation [69].

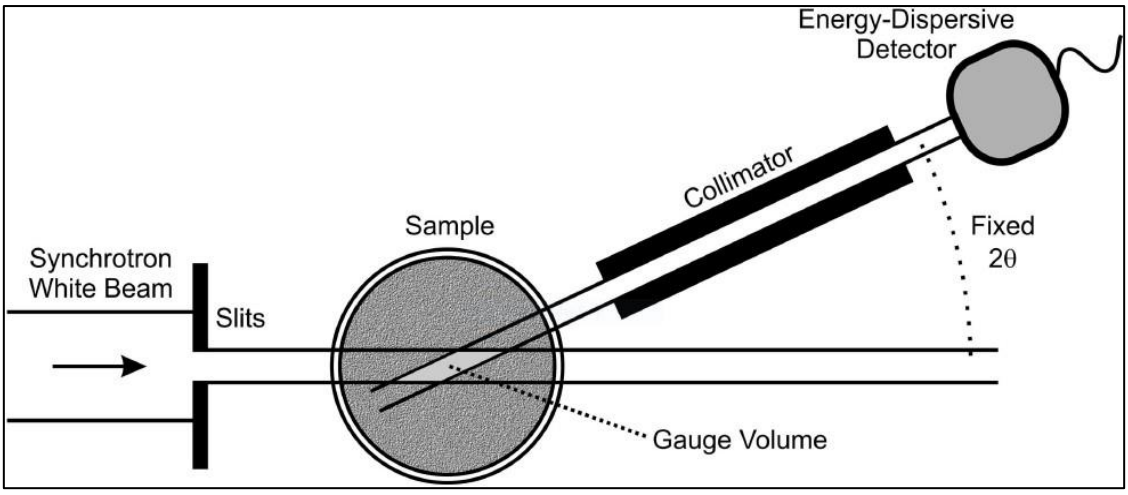

Figure II. 18: Schematic diagram of energy dispersive diffraction (EDD) technology.[68]

In the diffractometer, X-rays were produced from a CuKα radiation source with a wavelength of 1.540593 Å.

II.3.1.2. Determination of crystalline parameters

To calculate the crystalline parameter (cell parameter "a") of NiO thin layers the relationship between the inter-reticular distance of the planes (hkl) and the parameter was used crystallography [70]:

$$\frac{1}{dhkl^2} = \frac{h^2 + hk + k^2}{a^2} \quad \text{(II.5)}$$

II.3.1.3. Determination of crystalline size

With regard to the estimation of crystalline size of different samples fromdiffraction spectra, we used the Scherrer formula [71, 72]:

$$D = \frac{0.9\,\lambda}{\beta cos\theta} \quad \text{(II.6)}$$

D: the size of the crystals,

λ: the wavelength of the X-ray beam,

β: the half-height width of the diffraction line, expressed in radian (figure II.11),

θ: the diffraction angle.

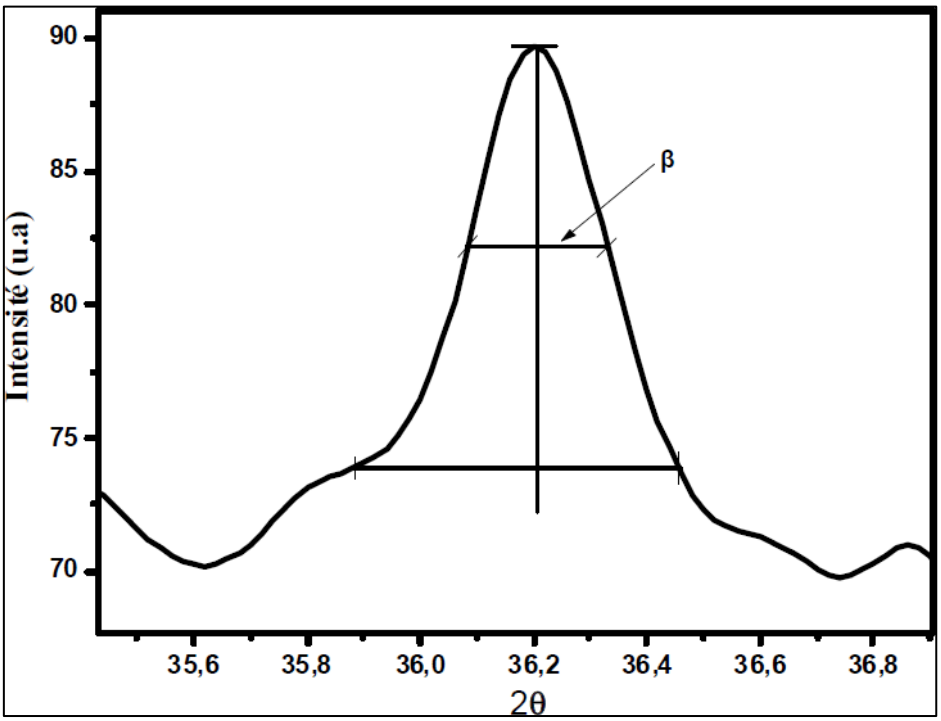

Figure II. 19: Illustration showing the definition of β (the half-height width of the X-ray diffraction line) [72].

II.3.1.4. Obtainable information from a diffract gram

• Qualitative analysis: Each crystal substance has a unique diffraction pattern. This may be thought of as the sample's fingerprint. By comparing the acquired data to the database, the material can be determined.

• Quantitative analysis: If the sample is not a pure material, but rather a mixture of multiple phases, the relative quantity of each phase may be determined.

• Lattice parameters: As previously stated, the crystal material is organised in a regular pattern. The material's unit cell is the smallest component of this regular structure. The size of the unit cell may be determined using XRD. This may be especially intriguing in non-ambient situations.

• Crystallite size and strain: The breadth of the obtained peaks is affected by the crystallite size of the powder. Broader peaks will be produced by crystallites smaller than 120 nm. This may be used to get data on the size of the crystallites. Peak broadening can also be caused by micro strain in the sample. Again, XRD measurements may be used to quantify this impact.

II.3.2. Electrical characterization

To directly know the surface resistance Rs, we used a four-point device (figure II.20). The probe consists of four aligned and regularly spaced contacts (figure II.21), A source supplies a current I flowing through the terminals exterior. The voltage U is measured at the terminals of the two inner tips. The use of four contacts instead of two, as in a classic resistance measurement, eliminates the need for tip resistance and only measures the resistance of the sample. When the distance "a" between the terminals is much greater than the thickness of the thin film "d", the lateral dimensions can be considered infinite. In this case, a two-dimensional model of conduction is considered:

$$\frac{U}{I} = K\frac{\rho}{d} \qquad \text{(II.7)}$$

ρ: the resistivity of the layer

d: the thickness.

The ratio characterizing this layer is represented by **RS** and **Ω**. For the readiness factor **K**, **R** is the ratio of voltage **U** to current **I**. Considering the cylindrical propagation of the field lines in the film, the coefficient **K** is **(ln2 /π)**.

From the relation (II.7), we have the formula (II.8) to deduce the resistivity of the four-point measurement knowing the thickness d of the thin film:

$$\rho = \left(\frac{\pi}{\ln 2} \times \frac{U}{I}\right) d = Rs \times d \qquad \text{(II.8)}$$

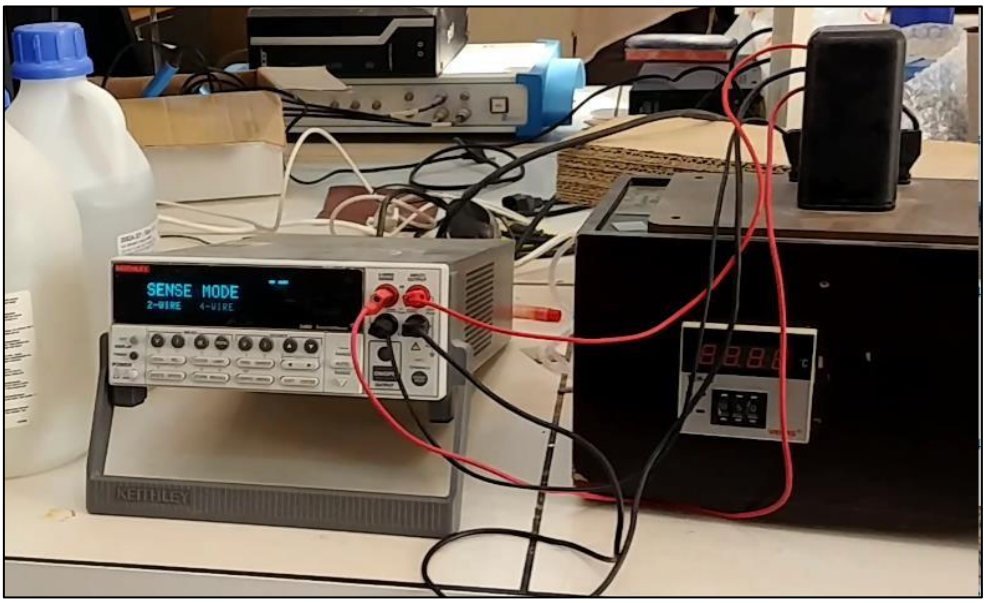

Figure II. 20: The experimental setup of the equipment using the four-probe method (Laboratory, Echahid Hamma Lakhdar University, ElOued).

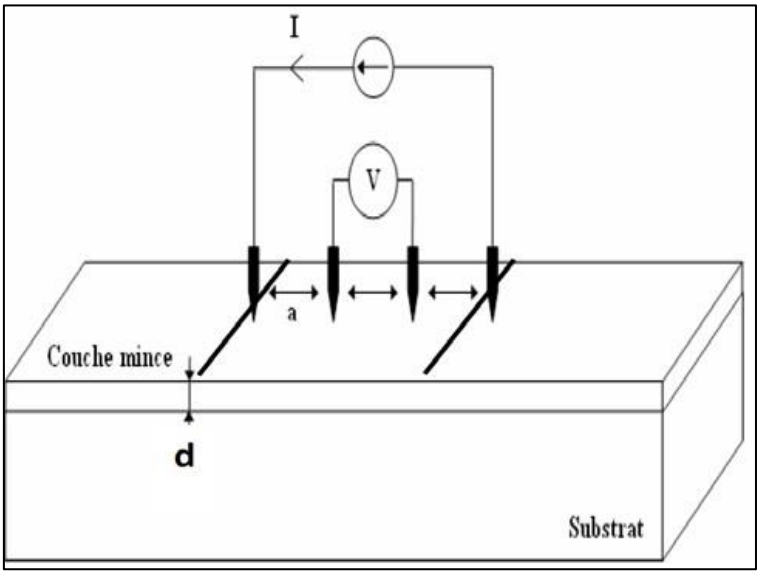

Figure II. 21: Diagram of a four-point device [68].

II.3.3. Optical characterization

Many of the parameters are characterised using optical techniques. They have the benefit over electrical techniques in that they are non-destructive and do not need chemical interactions to respond.

Optical techniques are classified into two categories:

• Methods for investigating the optical response of a material to stimulation, such as photo and cathode-luminescence.

• Methods for analysing the optical characteristics of a material, such as transmittance and reflectance measurements.

• The optical refractive index, material thickness, and optical gap are all determined by these spectroscopic measurements.

II.3.3.1. UV-Visible spectroscopy

The function of optical measuring equipment (Figure II.22) is based on the observation of changes and effects produced by electromagnetic radiation and matter interaction. From a technological standpoint, this entails producing electromagnetic radiation, changing its properties, and regulating its dispersion in a particular area. Similarly, the "fingerprint" left by the substance on the radiation must be generated in an understandable format (Figure II.23). [73]

Figure II. 22: Experimental UV-visible spectroscopy device used (organic materials laboratory. Echahid Hamma Lakhdar University).

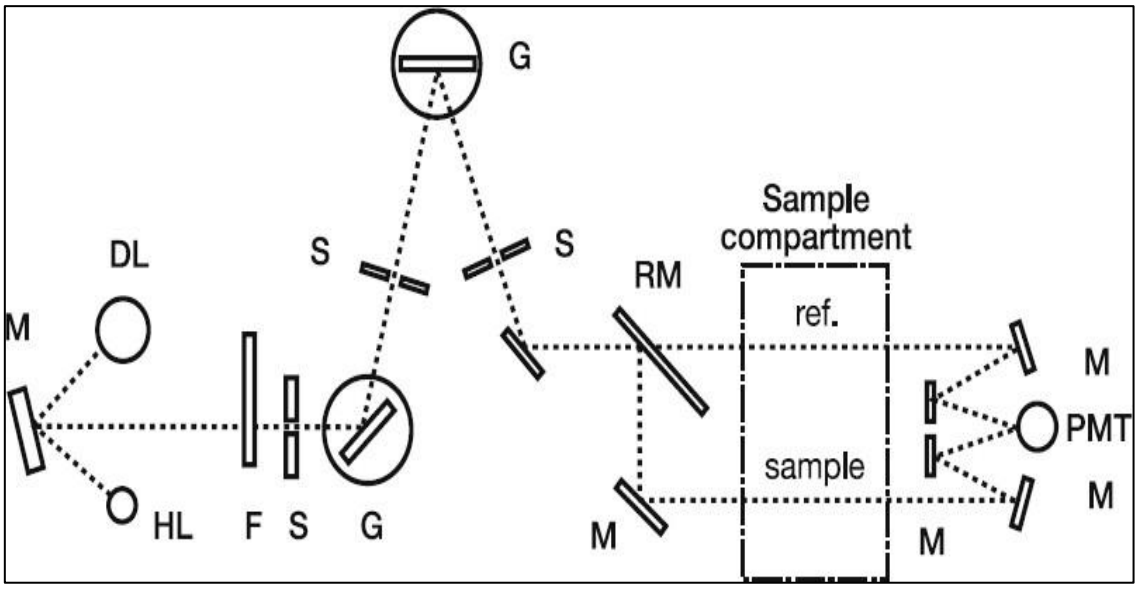

Figure II. 23: The layout of an imaginary spectrophotometer [75].

The light path is indicated by a dashed line. The components are represented as follows:

HL = halogen lamp.

DL = deuterium lamp.

M = mirror.

F = filter wheel.

S = slit.

G = grating.

RM = rotating mirror.

PMT = detector (photomultiplier tube)

II.3.3.2. Determination of the optical gap

The NiO material has a direct gap. Therefore, the expression of the coefficient absorption (α) as a function of the optical gap (Eg) and the energy (hν) of the photons is written under the form (Tauc equation) [76]:

$$\alpha hv = (hv - Eg) \quad \text{(II.9)}$$

Where:

A: a constant,

Eg: the bandwidth prohibited (or optical gap expressed in eV).

$h\upsilon$: the energy of a photon in eV.

α: the absorption coefficient.

n: equals 1/2 for permitted straight transition. Extrapolating the linear area of the (hv)2 against hv plot[56] yields the optical band gap energy value Eg.

II.3.3.3. Determination of Urbachenergy

In the field of optical properties, we calculated the energy of Urbach (Eu) to determine the state of disorder of the material. Indeed, the absorption coefficient, according to the law of Urbach, is given by the relation [78, 79]:

$$\alpha = \alpha_0 + \exp(\frac{h\upsilon}{E_u}) \quad \text{(II.10)}$$

α: is the absorption coefficient.

E: is the photon energy and is equal to

hv: is the Urbach energy.

II.4. Conclusion

In this chapter we have recalled the principle of deposit by Spray solar and then presented the deposit system that we carried out in the laboratory, and described the different characterization techniques used to analyze and determine the different structural properties, optical and electrical thin film of NiO

Chapter III:

Results and Discussion

Chapter III: Results and Discussion

III.1. Introduction

In this chapter, NiO thin films were formed on heated glass substrates at varied temperatures (350–375–400–425 and 450 °C) using the spray pyrolysis process. The physical characteristics of deposited NiO thin films were studied using an X-ray diffractometer (XRD), a UV-vis spectrophotometer, and a four probe technique.

III.2. Results and discussion

The structural characterizations were carried out using X-ray diffraction (XRD) with an X diffractometer (BRUKER-AXS type D8) equipped with a CuK radiation source, with a wavelength of 1.540593, and a scanning range of (2) of 25 to 55 °.

A UV-visible spectrophotometer was used to test the optical transmittance of the deposited thin films in the range of 300 to 900 nm (SHUMATZU 1800).

To validate the conduction and its change with precursor concentration, the effect Seebeck and four-point probe were used to 2 x 1 cm papers for all samples.

III.2.1. Structural properties

X-ray diffraction (XRD) patterns of NiO thin films were recorded by spray pyrolysis at various temperatures 350, 375, 400, 425 and 450, and they are shown in **Figure III.1**.structural operations.

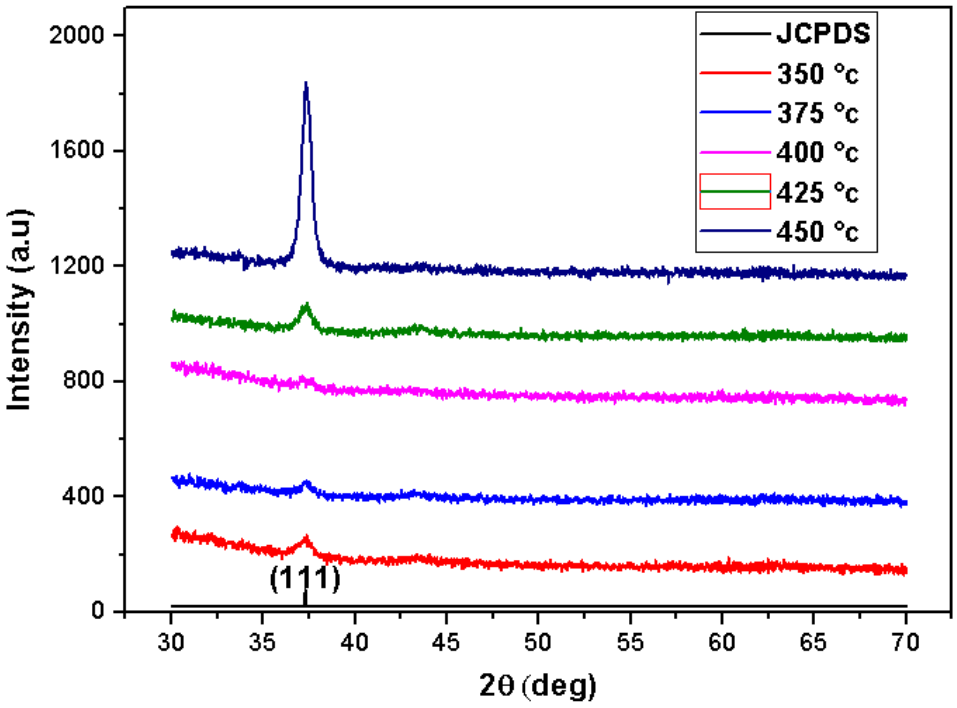

Figure III. 1: X-ray diffraction patterns of NiO films deposited at different substrate temperatures.

III.2.1.1. X-Ray Diffraction Studies:

The X-ray diffraction patterns of NiO thin films at various substrate temperatures (350–450 °C) are shown in Figure III.1. All LMS phi structures are polycrystalline, with a cubic phase (bun-senite, JCPDS 004-0835) that preferentially aligns along with the (1 1 1) directions. For all deposition temperatures corresponding to the cubic structure of NiO, the (1 1 1) peak is about 37.3. The observed unit cell parameter reflects the conventional unit cell characteristics. Table I displays the microscopic characteristics of NiO thin blocks produced at various substrate temperatures.

Here, k = 0.94 is the form factor, k is the X-ray wavelength utilised (here, k = 1.513), is the full width at half maximum (FWHM) of the associated peak, and h is the Bragg angle, thus; the planes' crystalline size (1 1 1) was determined. The average crystal size grew from 7 nm to 18 nm when the substrate temperature rose from 400 to 450 °C. This may be due to an increase in crystalline quality as the substrate temperature rises. The results of an XRD analysis include structural characteristics such as crystals per unit area (N), microstrain (e), and dislocation density (d).

The following equation is used to calculate the mesh parameter a for NiO in a cubic structure:

$$\frac{1}{d_{hkl}^2} = \frac{h^2+k^2+l^2}{a^2} \quad \text{(III.1)}$$

Where hkl are the Miller indices and dhkl is the inter-reticular spacing as determined by Bragg's law:

$$2d_{hkl} \sin\theta = n\lambda \quad \text{(III.2)}$$

Where n is the diffraction order (first order), λ is the wavelength of the radiation (λ = 1.540593 A) for the CuKa radiation, θ and is the Bragg diffraction angle of peak in radians. Utilizing the Scherrer equation, the grain measurement D of the films was determined for the (111) plane:

$$D = \frac{0.9}{\beta \cos\theta_{hkl}} \quad \text{(III.3)}$$

If β is the diffraction angle's full width at half height (FWHM), λ is the incoming radiation's X-ray wavelength (1.540593 A °).

The averaged stress ε in NiO thin films can be calculated using the following formula:

$$\varepsilon = \frac{a-a_0}{a_0} \times 100\% \quad \text{(III.4)}$$

Where a and a0 are the mesh parameters of NiO thin films, the core material's standard mesh parameter is (a0 = 4.1769 A °) according to the standard map (JCPDS, number004-0835).

The dislocation density, defined as the number of dislocation lines per unit volume, was determined using the following formula [82]:

$$\delta = \frac{1}{D^2} \quad \text{(III.5)}$$

Table III. 1: In which optical band gap energy (Eg) of the NiO thin film, computed using transmittance, is shown.

Temperature (°c)	2θ (deg)	interplanar spacing dhkl (A°)	Latice Constants (A°)	β (deg) FWHM	D (nm)	lattice strain (%)	δ x 1015 (lines/m2)
350	**37.292**	**2.409**	**4.173**	**0.672**	**12.6**	**0.869**	**6.299**
375	**37.013**	**2.408**	**4.171**	**0.912**	**9.3**	**1.189**	**11.562**
400	**37.329**	**2.407**	**4.169**	**1.152**	**7.3**	**1.488**	**18.765**
425	**37.427**	**2.403**	**4.162**	**0.551**	**15.4**	**0.71**	**4.217**
450	**37.314**	**2.408**	**4.171**	**0.48**	**17.8**	**0.62**	**3.156**

III.2.1.2. Optical properties

Figure III.2 shows the optical depletion of NiO thin films at different temperatures of the substrate. The permeability of the thin NiO particles is improved with the temperature of the substrate.

The elevation in the intensity of the penetration coefficient with therising substrate temperature may be attributed to the intensification of the lms defect. The latter is thin film NiO refractive index (n).

We note from the model that, at 400 degrees, the penetration was as large as 76.9%, but at 450 degrees, the penetration was as little as 54.5%.

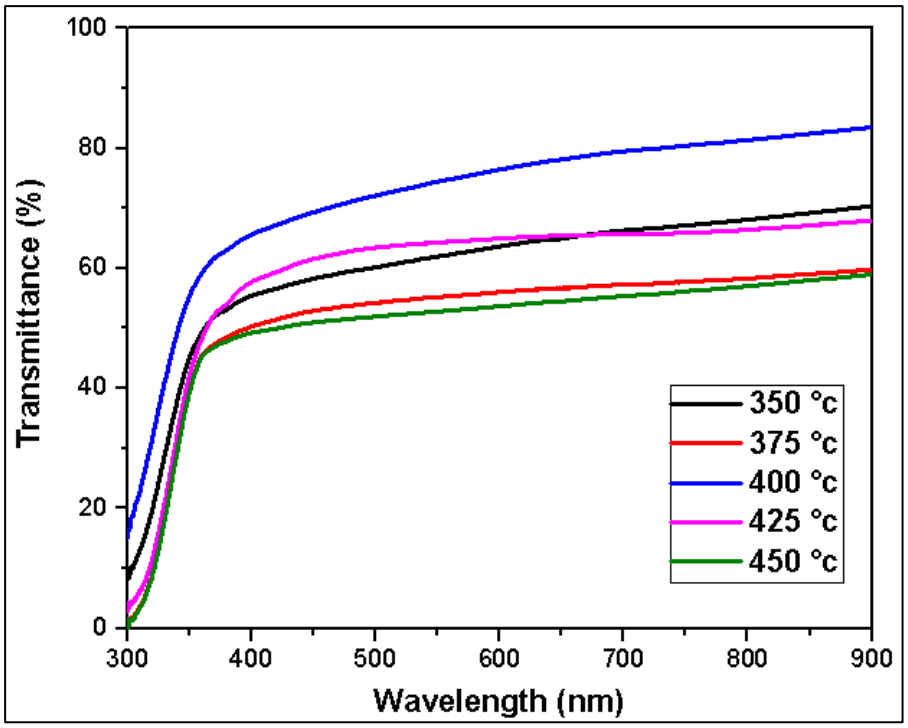

Figure III. 2: transmittance layers at temperatures different from the substrate.

Table III. 2: Values of thickness t, mean transmittance, optical bandgap energy and Urbach energy Eu of thin films of NiO prepared at different temperatures.

Temperature (°C)	Thickness (nm)	Average Transmittance (%)	Gap Energy Eg(eV)	Urbach EnergyEu (meV)
350	176.99	64.2	3.68	466
375	204.46	56.3	3.72	343
400	137.67	76.9	3.66	478
425	187.71	64.8	3.71	362
450	211.58	54.5	3.74	334

The absorption coefficient (α) of thin NiO films was obtained from transmittance measures using the Swanepoel technique [83, 84] for any further research:

$$\alpha = \frac{1}{t}\ln\frac{1}{T} \quad \text{(III.6)}$$

Where t and T are the layer's thickness and transmittance, respectively, t he energy gap values are usually determined by the layer's crystal structure (disorder and regularity). Also, as seen in Tauc's equation, (α) and incoming photon energy ($h\upsilon$) are related:

$$(\alpha h\upsilon) = A(h\upsilon - E_g)^n \quad \text{(III.7)}$$

The optical band gap energy (Eg) of the NiO thin film, computed using transmittance, is shown in Figure III.3.

Where Eg is the band gap and α is the absorption coefficient,, ht is the energy of the photon, A is constant and n assumes the values of 1/2, 2, 3/2 and 3 for the permissible direct, indirect permissible ratio, Forbidden indirect transformations and direct forbidden transformations, respectively. The band gap is raised from 3.68 eV to 3.74 eV.

The temperature of the different substrate decreased remarkably at an average temperature (400 ° C). The obtained bandgap values are well consistent with previously reported data.

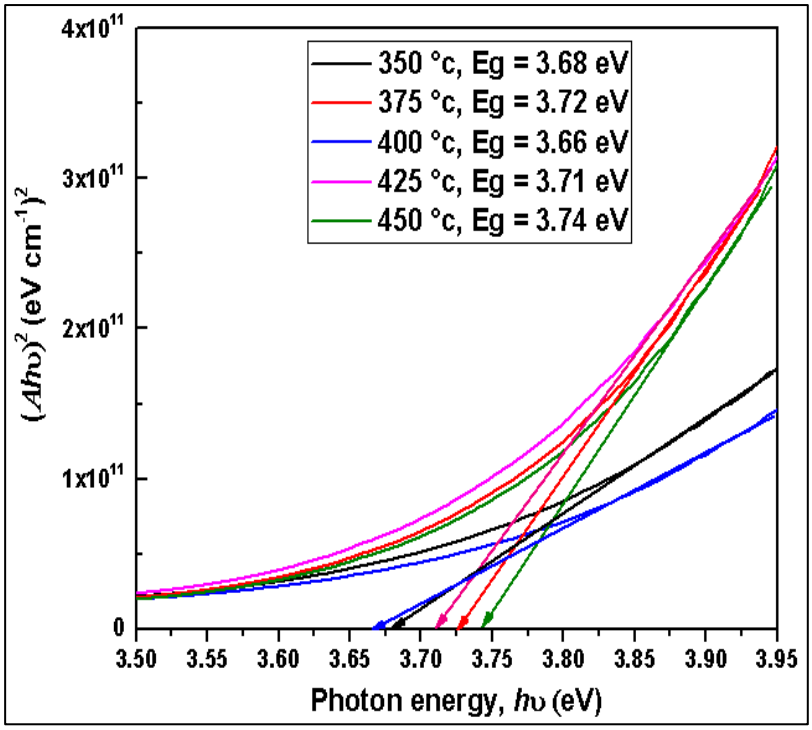

Figure III. 3: Estimation of the optical gap (Eg) from the Tauc relation compared to thin layers of NiO prepared at different ° C

Table III.2 shows the computed band gap values. The band gap values obtained match well with the findings of the literature [85, 86]. Urbach tail, a disorder linked to the localised states accessible of width in the optical band gap of thin NiO films and influencing their structure, was created for further study. This localised state width is closely linked to a comparable exponential tail for the density of states at the band's borders and can be stated as follows:

$$\alpha = \alpha_0 \exp(\frac{h\upsilon}{E_u}) \quad \text{(III.8)}$$

Figure III.4 depicts the contrast against photon energy (Eu) of the films. The values were obtained by taking the reciprocal of the straight line slopes, as shown in **(Figure. III.4)**, and as indicated in (Table), the average power band gap was estimated to be (334 – 466 meV). The reduction in the visible range gap may be attributable to winds related to higher grain size and decreased structural disturbances in the films, as seen by Urbach energy analysis.

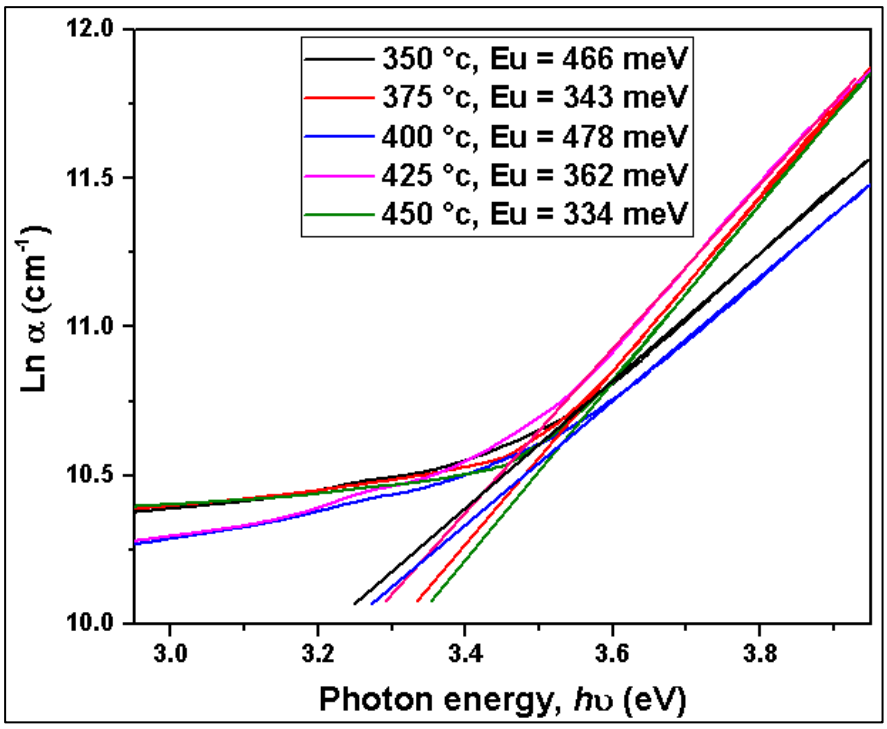

Figure III. 4: Anisotropy of lnα as a function of hυ to determine the Urbach tail energy for thin layers of NiO prepared at different ° C.

In **Figure III.5**, a comparison of the differences in optical bandwidth and Urbach energy for thin films as a function of temperature is given. In general, it is observed that the previous two parameters differ in the opposite direction of temperature. Indicates an increase in the value of Urbach energy (with a decrease in temperature)

We notice a decrease in the value of the Gap, with a value of 3.66, and the highest values of 3.74, and vice versa in the value of

Urbach, with a maximum value of 0.45 V and a minimum of 0.33 V, indicates that the layer has fewer defects and therefore a decrease in the optical gap, and this gives us good transparency of the layer.

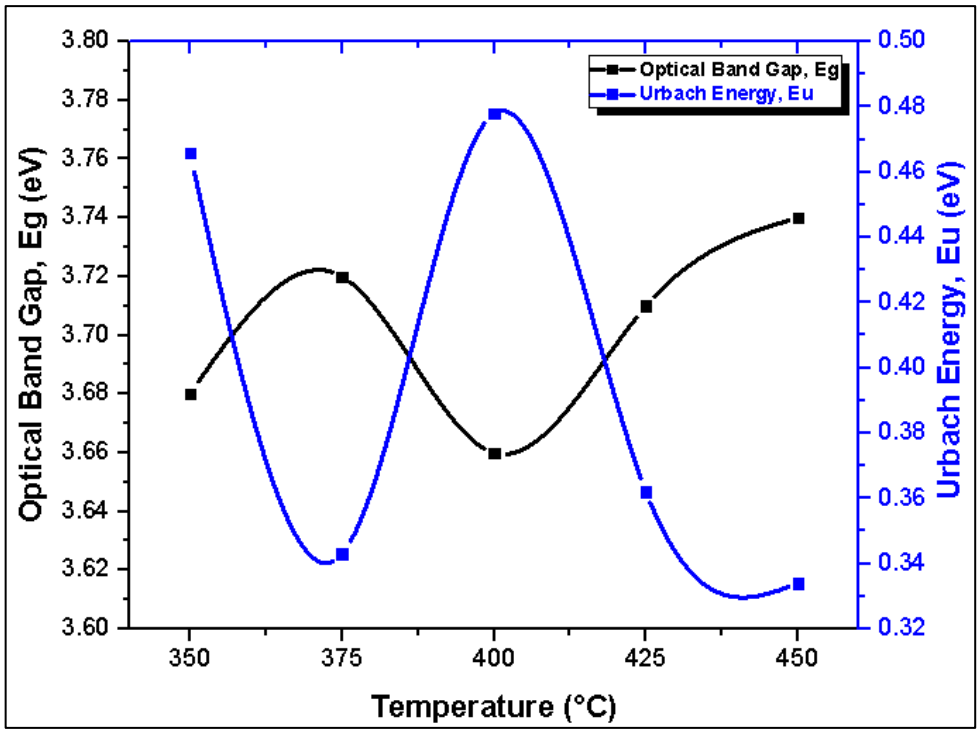

Figure III. 5: Comparison of optical gap values and Urbach energy values for thin films (NiO) as a function of temperature.

III.2.1.3. Electrical properties

It should be mentioned that NiO is recognised as a p-type semiconductor owing to the observed defect of p-type conductivity, vacancies in Ni + 2 [87]. All samples were subjected to the Seebek effect, and p-type conductivity was verified. A four-point probewas used to determine electrical conductivity at room temperature.

The development of electrical conductivity and thickness of NiO films as a function of solution temperature is shown in **Figure III.6**. This curve demonstrates that the conductivity of the samples decreases as the thickness of the NiO films increases with the increase in the temperature of the solution, and the conductivity increases as the thickness of the films decreases, indicating a “direct ratio,” with the highest conductivity value being 0.0055 $(ohm\ cm)^{-1}$.

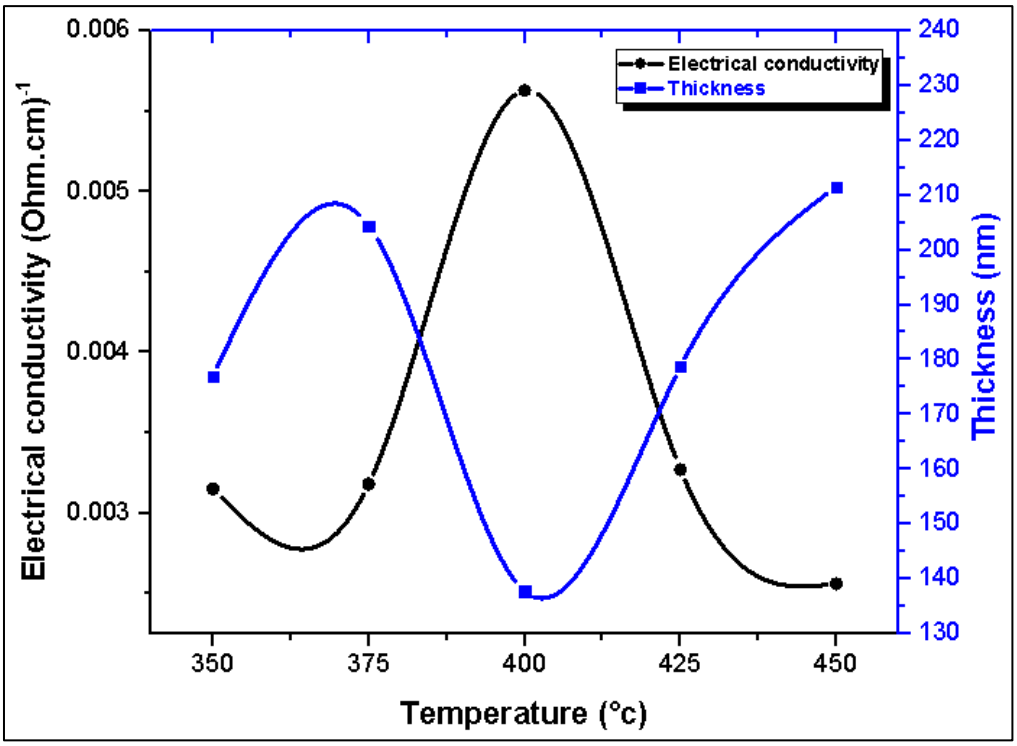

Figure III. 6: Differences in conductivity and thickness (t) of thin NiO films as a function of different temperatures

III.3. Conclusions

In this separation, the NiO thin-film particles were condensed into a substrate at different temperatures. Spray pyrolysis technology has been used, which is easy to use and affordable (inorganic solution). Structural electro-optical properties have been applied. The XRD patterns showed that the structure of the NiO film is still in the preferred (111) orientation. This was consistent across all substrate temperatures. The results showed the best surface morphology at high temperatures up to 17.8 nm. This was particularly the case at 400 °C as shown in the figure. Analytical studies have shown that all nickel particles contain nickel and oxygen. The optical gap was significantly changed (3.68 eV to 3.74). The refractive index, extinction coefficient, and the substrate temperature had an effect on the real and hypothetical dielectric constants, as well as the optical conductivities of NiO films. Electrical investigations have shown that NiO thin films are semiconducting in nature.

General conclusion

General conclusion

A lot of work focuses on the development and use of metal oxide thin layers with different deposition techniques and patterns, in which various factors and deposition conditions characteristic changes in various applications in the electronics and optical industries have been studied. In this context, we studied the effects of temperature on the structure, optical and electrical properties of nickel films, because we developed them using a solar furnace at different temperatures through spray pyrolysis on glass substrates.

We start by comprehending the sun's structure and properties, then moving to the energy it provides. We also discuss the topic of solar energy and its use in Algeria. The solar collector pan is thus characterised as an oven capable of producing thin films. Furthermore, we explore NiO film's structure, electronic, electrical, and optical properties. In addition, we cover thin film deposition as well as the spray pyrolysis deposition concept.

In this case, the purpose of this work is to study the effect of temperature changes on the properties of nickel oxide (NiO) films (structure, optical and electrical). We use solar furnaces at different temperatures (350 c°, 375 c°, 400 c°, 425 c°, and 450 c°) to develop nickel oxide thin films on heated glass substrates with a molar concentration of 0.1 mol/L through the spray pyrolysis solar method. Layer, used to spray a solution containing nickel nitrate hexahydrate (Ni (NO3) 2 .6H2O) dissolved in distilled water. From it, we demonstrated the deposition system we fabricated in the laboratory and described the different characterization techniques used to analyze and quantify the properties of different structures, namely the optical and electrical thin films of NiO.

We condense the NiO film particles in the substrate at different temperatures. Using spray pyrolysis technology, easy to use, affordable (inorganic solution). Electro-optical structure characteristics have been applied. The XRD pattern shows that the structure of the NiO film is still in the preferred (111) orientation. This is consistent across all substrate temperatures. The results show better surface morphology at higher temperatures. this is especially true at 400 °C. Analytical studies have shown that all nickel particles contain nickel and oxygen. The optical gap has changed significantly (3.68 eV to 3.74). The refractive index, extinction coefficient, real and imaginary dielectric constants, and optical conductivity of the NiO film are all affected by the temperature of the substrate. Electrical studies of NiO films show that they are semi-conducting in nature.

Finally. We are looking forward to re-applying the experiment again, using other metals or changing the molar concentration.

References

References

[1] Space, What Is Our Sun Made Of? Space.com: //www.space.com/14745-sun-composition.html, (2012, March 1).

[2] NASA, Sun Fact Sheet [Online] Available: https://nssdc.gsfc.nasa.gov/planetary/factsheet/sunfact.html. (August 4, 2015).

[3] NASA Goddard Space Flight Center, The Sun [Online]. Available: https://www.flickr.com/photos/gsfc/, (July 30, 2015).

[4] Jump up to: 4.0 4.1 What You Need to Know About Energy, Our Energy Sources: The Sun [Online]. Available: http://needtoknow.nas.edu/energy/energy-sources/the-sun/, (July 31, 2015)

[5] ITACA, The Sun as a Source of Energy [Online]. Available: http://www.itacanet.org/the-sun-as-a-source-of-energy/part-2-solar-energy-reaching-the-earths-surface/, (August 4, 2015).

[6] B. Amar Mohammed, https://www.aljazeera.net/blogs/2018/8/29/الطاقات-المتجددة-بالجزائر-البديل, (2018, August 29)

[7] A. Messai, Y. Benkedda, S. Bouaichaoui, and M. J. E. P. Benzerga, "Feasibility study of parabolic trough solar power plant under Algerian climate," vol. 42, pp. 73-82, 2013.

[8] Hancock, N, Solar Water Distillation. Safe Drinking Water Foundation. https://www.safewater.org/fact-sheets-1/2016/12/8/solar-water-distillation. (2019, February 22)

[9] Solar Drying. Solar Drying - an overview | ScienceDirect Topics. (n.d.). https://www.sciencedirect.com/topics/engineering/solar-drying, Renewable and Sustainable Energy Reviews, 2018

[10] What is solar cooking? One Earth Designs Inc. (n.d.). http://www.oneearthdesigns.org/what-is-solar-cooking/.

[11] L. Tomasini, Les traitements de surface sous vide, (SOLLAC, Groupe Usinor), La Revue de Métallurgie - CIT Avril (2001).

[12] C.V. Thompson, Secondary grain growth in thin films of semiconductors: theoretical aspects, J. Appl. Phys. Vol.58, 763, (1985).

[13] O. Daranfad, Elaboration et caractérisation des couches minces de Zinc préparé par spray ultrasonique, Mémoire de Magister, University Mentouri, Constantine, (2007).

[14] H.J. Frost, C.V. Thompson, Computer simulation of microstructural evolution in thin films, J. Elec. Mater.Vol.17, 447, (1988).

[15] C.V. Thompson, Grain growth in thin films, Mater. Sci. Vol.20 245-268, (1990).

[16] S. Andrieu, “Introduction aux couches minces et réseau”. School Franco-Roumaine: Magnétisme des systèmes nanoscopiques et structures hybrides-Brasov, (2003).

[17] Boudrifa Ouassila, "Mecanisme De Formation De Couches Minces De Fer- Nickel Obtenues Par Pvd", Magister Thesis, University Ferhat Abbas–SETIF, 2010.

[18] M. V. Nikoli´c, V. Blagojevi, K. M. Paraskevopoulos, T. T. Zorba , D. Vasiljevi-Radovi, P. M. Nikoli and M. M. Risti, "Far infrared properties of sintered NiO", Journal of the European Ceramic Society, Vol. 27, 469–474, (2007).

[19] H. Benzscour, "Synthèse d’un oxyde transparent conducteur (OTC) par pulvérisation chimique (ZnO, NiO)", Magistere Thesis, Badji Mokhtar University, Algeria, (2008).

[20] S. Perusin, "Conséquences de l'oxydation haut température sur l'injection de défauts et le comportement mécanique des matériaux métalliques", Doctoral Thesis, Toulouse University, France, (2004).

[21] J. D. Desai, S. K Min, K. D. Jung and O. S. Joo, "Spray pyrolytic synthesis of large area NiOx thin films from aqueous nickel acetate solutions", Applied Surface Science, Vol. 253, No. 4, 1781-1786, (2006).

[22] P. D. Hoon, "Optimization of nickel oxide-based electrochromic thin films", Doctoral Thesis, Bordeaux 1 University, France, (2010).

[23] I. E. Britannica, Encyclopaedia britannica. Encyclopaedia Britannica, Incorporated, 1957.

[24] N. Greenwood and A. Earnshaw, Chemistry of the Elements 2nd Edition. Butterworth-Heinemann, 1997.

[25] E. Thimsen, A. B. Martinson, J. W. Elam, and M. J. Pellin, "Energy levels, electronic properties, and rectification in ultrathin p-NiO films synthesized by atomic layer

deposition," The Journal of Physical Chemistry C, vol. 116, no. 32, pp. 16830-16840, 2012.

[26] V. Marcio, P. S. Renan and I. C. Susana, "Synthesis and characterization of stable Co and Cd doped nickel hydroxide nanoparticles for electrochemical applications", Ultrasonics Sonochemistry, Vol. 16, No.1, 35-40, (2009).

[27] P. S. Patil, L. D. Kadam, "Preparation and characterization of spray pyrolyzed nickel oxide (NiO) thin films", Applied Surface Science, Vol. 199, 211-221, (2002).

[28] H. Benzscour, "Synthèse d'un oxyde transparent conducteur (OTC) par pulvérisation chimique (ZnO, NiO)", Magistere Thesis, Badji Mokhtar University, Algeria, (2008).

[29] S. Stanescu, "Les 'glissements de type écoulement' dans les marnes noires des Alpes du Sud. Morphologie, fonctionnement et modélisation hydro-mécanique", Doctorat Thesis, Louis Pasteur – StrasbourgI University, France, (2002).

[30] T. M. Schuler, D. L. Ederer, S. Itza-Ortiz, G. T. Woods, T. A. Callcott and J. C. Woicik, "Character of the insulating state in NiO: A mixture of charge transfer and Mott-Hubbard character", Phys. Rev. B - Condens. Matter Mater. Phys., Vol. 71, No. 11, 1-7, (2005).

[31] N. F. Mott, "The basis of the electron theory of metals, with special reference to the transition metals", Proceedings of the Physical Society. Section A, Vol. 62, No. 7, 416-422, (1949).

[32] J. Hubbard, "Exchange splitting in ferromagnetic nickel", Proceedings of the Physical Society, Vol. 84, No. 4, 55-464, (1964).

[33] S. Lany, J. Osorio-Guillén and A. Zunger, "Origins of the doping asymmetry in oxides: Hole doping in NiO versus electron doping in ZnO", Phys. Rev. B -Condens. Matter Mater. Phys., Vol. 75, No. 24, 1-4, (2007).

[34] B. E. Saracin, "Structural and optoelectronic properties of sol-gel derived nickel oxide thin films", Doctoral Thesis, Middle East Technical University, Turkey, (2017).

[35] Sadani Younes, Slimani Soufiane and Kouidi Tarek, "Exploitation and use of solar energy to Synthesis and characterization of Pure and Cobalt-doped NiO Nanoparticles by spray pyrolysis", Master Thesis, Echahid Hamma Lakhdar University of El-Oued, Algeria, (2020).

[36] G. A. Sawatzky and J. W. Allen, "Magnitude and origin of the band gap in NiO", Physical Review Letters, Vol. 53, No. 24, 2339-2342, (1984).

[37] P. Lunkenheimer, A. Loidl, C. R. Ottermann, and K. Bange, "Correlated barrier hopping in NiO films", Physical Review B, Vol. 44, No. 11, 5927-5930, (1991).

[38] Z. Zhiwie, Oxygen reduction lithiated nickel oxide as catalyst and catalyst support, PhD thesis case Western Reserve University, 1993.

[39] G. Williams and G. S. V. Coles, "The Gas-Sensing Potential of Nanocrystalline Tin Dioxide Produced by a Laser Ablation Technique", MRS Bulletin, Vol. 24, No. 6, 25-29, (1999).

[40] David C. Look, D. C. Reynolds, C. W. Litton, R. L. Jones, D. B. Eason, and G. Cantwell, "Characterization of homoepitaxial p-type ZnO grown by molecular beam epitaxy", Applied Physics Letter, Vol. 81, No. 10,1830-1832, (2002).

[41] A. M. Reddya, A. S. Reddyb and P. S. Reddya, "Annealing effect on the physical properties of dc reactive magnetron sputtered nickel oxide thin films", Physics Procedia, Vol. 49, 9-14, (2013).

[42] P.J. Kelly and R.D. Arnell, "Magnetron sputtering: a review of recent developments and applications", Vacuum, Vol. 56, 159-172, (2000).

[43] M. Leskelä, and M. Ritala, "Atomic layer deposition (ALD): from precursors to thin film structures". Thin Solid Films, Vol. 409, No. 1, 138-146, (2002).

[44] D. Perednis and L. J. Gauckler, "Thin film deposition using spray pyrolysis", Journal of Electroceramics, Vol. 14, 103-111, (2005).

[45] S. A. Mahmoud, S. Alshomer and M. A. Tarawnh, "Structural and optical dispersion characterization of sprayed Nickel Oxide thin films", Journal of Modern Physics, Vol. 2, 1178-1186, (2011).

[46] R. C. Korošec and P. Bukovec, "Sol-Gel Prepared NiO thin films for electrochromic applications", Acta Chim. Slov, Vol. 53, 136-147, (2006).

[47] F. Y. Yang, Kai Liu, Kimin Hong, D. H. Reich, P. C. Searson and C. L. Chien" Large magnetoresistance of electrodeposited Single-Crystal Bismuth thin films", Science, Vol. 284, No. 5418, 1335-1337, (1999).

[48] J. C. Osuwa and G. I. Onyejiuwa, "Structural and electrical properties of annealed Nickel Oxide (NiO) Thin Films preapared by chemical bath deposition", Journal of Ovonic Research, Vol. 9, No. 1, 9-15, (2013).

[49] Y.Z. Liu, C.C. Wang and M. Chu, "Low threshold 1.3-μm InGaAsP/InP lasers prepared by a single-step liquid-phase epitaxy", Journal of Applied Physics, Vol. 63, 2151-2151, (1988).

[50] D. J. Estes and M. Mayer, "Electroformation of giant liposomes from spin-coated films of lipids", Colloids and Surfaces B: Biointerfaces, Vol. 42, 115-123, (2005).

[51] P. Baudry, A. C. M. Rodrigues, M. A. Aegerter and L. O. Bulhões, "Dip-coated TiO2-CeO2 films as transparent counter-electrode for transmissive electrochromic devices". Journal of Non-Crystalline Solids, Vol. 121, 319-322, (1990).

[52] H. Amani Hamedani, "Investigation of deposition parameters in ultrasonic spray pyrolysis for fabrication of solid oxide fuel cell cathode," Georgia Institute of Technology, 2008.

[53] D. M. Mattox, "Physical vapor deposition (PVD) processes," Metal Finishing, vol. 100, pp. 394-408, 2002.

[54] X.-T. Yan and Y. Xu, Chemical vapour deposition: an integrated engineering design for advanced materials. Springer Science & Business Media, 2010.

[55] H. O. Pierson, Handbook of chemical vapor deposition: principles, technology and applications. William Andrew, 1999.

[56] J. Creighton and P. Ho, "Introduction to chemical vapor deposition (CVD)," Chemical vapor deposition, vol. 2, pp. 1-22, 2001.

[57] A. Hunt, W. Carter, and J. Cochran Jr, "Combustion chemical vapor deposition: A novel thin-film deposition technique," Applied Physics Letters, vol. 63, no. 2, pp. 266-268, 1993.

[58] Y. Xu and X.-T. Yan, "Introduction to chemical vapour deposition," Chemical Vapour Deposition: An Integrated Engineering Design for Advanced Materials, pp. 1-28, 2010.

[59] M. A. Mahadik, , Degradation of organic impurities in water using nanocrystalline ferric oxide semiconductor thin films, PhD thesis, Shivaji University, 2014.

[60] G. Korotcenkov, V. Brinzari, J. Schwank, M. DiBattista, and A. Vasiliev, "Peculiarities of SnO2 thin film deposition by spray pyrolysis for gas sensor application," Sensors and Actuators B: Chemical, vol. 77, no. 1-2, pp. 244-252, 2001.

[61] K. M. Jadhav, Structural electrical optical and magnetic properties of some ferrite thin film prepared by spray pyrolysis technique, PhD thesis, Babasaheb Ambedkar Marathwada University, 2017.

[62] Y.Aoun, "Conception et développement d'un four solaire pour l'élaboration des oxydes métalliques – caractérisation des oxydes", PhD Thesis, University of Mohamed khider-Biskra, (2016).

[63] S.Younes, S. Soufiane, K.Tarek"Exploitation and use of solar energy to Synthesis and characterization of Pure and Cobalt-doped NiO Nanoparticles by spray pyrolysis"2020.

[64] V. Neeranartvong, Etude d'un concentrateur solaire à simple réflexion. Thèse de Docteur, Ingenieur, Institut National Polytechnique, Toulouse, (1983).

[65] B.Y.H.Liu and R.C. Jordan, The interrelationship and characteristic distribution of distribution of direct, diffuse and total solar radiation, Solar Energy, (1960).

[66] K.Kamli, "Elaboration et caractérisations physico-chimique des couches minces de sulfure d'étain par spray ultrasonique: Effet des sources d'étain", Memory of Magister, Mohamed Khider-Biskra University, Algeria, 2013.

[67] Y. Waseda, E. Matsubara, and K. Shinoda, X-ray diffraction crystallography: introduction, examples and solved problems. Springer Science & Business Media, 2011.

[68] A. Le Bail et al., Powder diffraction: theory and practice. Royal society of chemistry, 2008.

[69] L. V. Azároff, R. Kaplow, N. Kato, R. J. Weiss, A. Wilson, and R. Young, X-ray Diffraction (no. 1). McGraw-Hill New York, 1974.

[70] H.Benzarouk, Synthèse d'un oxyde transparent conducteur (OTC) par pulvérisation chimique (ZnO, NiO), Master's thesis, University of Annaba (Algeria), (2008).

[71] H.Nanto, T.Minami, S.Takata, Phys. Stat. Sol. A. 65, K 131, 1981.

[72] S. Benramache, Elaboration et caractérisation des couches minces de ZnO dopées cobalt et indium, Doctoral thesis in science, Mohamed Khider University – Biskra (Algeria), 2012.

[73] K. Sakoda, Optical properties of photonic crystals. Springer Science & Business Media, 2004.

[74] Abdelbaki NID, kamal TOUATI HAMAD and Riadh FAR, L'effet de la molarité de nickel sur les propriétés des couches minces d'oxyde de nickel NiO élaborées par la technique de spray pyrolyse alimentée par énergie solaire," 2019.

[75] J. A. Räty, K.-E. Peiponen, and T. Asakura, UV-visible reflection spectroscopy of liquids. Springer Science & Business Media, 2004.

[76] S. Chelouche, Propriétés des fenêtres optiques ZnO:Al pour cellules solaires en couches minces à base de CIGS, Magister's thesis, Ferhat Abbas-Sétif University (Algeria), 2012.

[77] P. Dhamodharan, C. Manoharan, S. Dhanapandian, M. Bououdina, and S. Ramalingam, "Preparation and characterization of spray deposited Sn-doped ZnO thin films onto ITO subtracts as photoanode in dye sensitized solar cell," Journal of Materials Science: Materials in Electronics, vol. 26, no. 7, pp. 4830-4839, 2015.

[78] F. Bouabida, "Variation des propriétés structurales et optiques des couches minces de ZnO sous l'effet du temps de dépôts", Master's thesis, Larbi University Tebessi, Tebessa (Algeria), 2013.

[79] A. Bougrine, A. El Hichou, M. Addou, J. Ebothé, A. Kachouna, M. Troyon, Material Chemistry and Physics. 80, 438-445, 2003.

[80] Y. Benkhetta, "L'effet du débit de la solution sur les propriétés des couches minces d'oxyde de zinc (ZnO) déposées par spray ultrasonique," 2013.

[81] B. D. Berrouis Soumia, "Elaboration et caractérisation de couche mince NiO: Co."

[82] L. Smaoun, C. Bellagh, and N. Ait Ahmed, "Électrodéposition des couches minces de l'oxyde de nickel et étude de leur activité électro catalytique vis-à-vis de l'oxydation du Méthanol et du Propanol," University of Abderrahmane Mira-Bejaia, 2016.

[83] H. C. Casey Jr., D. D. Sell, and K. W. Wecht, Concentration dependence of the absorption coefficient for n- and p-type GaAs between 1.3 and 1.6 eV, Journal of Applied Physics, vol. 46, no. 1, pp. 250–257, 1975.

[84] R. Y. Mohammed, S. Abduol, and A. M. Mousa, Correlation between optical and structural properties of chemically deposited cds thin films, International Letters of Chemistry, Physics and Astronomy, vol. 11, pp. 146–158, 2014.

[85] J.D.Desai, S.-K.Min,K.-D.Jung,andO.-S.Joo,"Spraypyrolytic synthesis of large area NiOx thin films from aqueous nickel acetate solutions," Applied Surface Science, vol. 253, no. 4, pp. 1781–1786, 2006.

[86] H. A. Juybari, M.-M. Bagheri-Mohagheghi, and M. ShokoohSaremi, Nickel-lithium oxide alloy transparent conducting films deposited by spray pyrolysis technique, Journal of Alloys and Compounds, vol. 509, no. 6, pp. 2770–2775, 2011.

[87] P. Mohanty, C. Rath, P. Mallick, R. Biswal, and N. C. Mishra, UV-visible studies of nickel oxide thin film grown by thermaloxidation of nickel, Physica B: Condensed Matter, vol. 405, no. 12, pp. 2711–2714, 2010.

Abstract

The goal of this research was to use solar energy to create a thin Nickel Nitrates film (NiO) using the Spray Pyrolysis solar method, as well as to investigate the impact of altering the temperature on the thin film's (structural, optical, and electrical) characteristics. Where Ni (NO3) 2 6H2O has been used. Thin films with a molar concentration of 0.1 mol/L are placed on a glass substrate and utilising a sun oven at various heat temperatures (350 c°, 375 c°, 400 c°, 425 c°, and 450 c°). X-Ray Crystallography (structural characteristics), Ultraviolet–visible spectroscopy (optical properties), and the Four Probe Method were used to examine the characteristics of the thin films (Electrical properties). The materials crystallise in a cubic form, according to the Ultraviolet–visible spectroscopy study. As the film density declines, the thin film crystals follow a preferred orientation (1 1 1), with the spacing between the particles reaching a maximum of 37.7 nm at 450 C°. While UV–visible spectroscopy revealed that the film's permeability rose at a temperature of 400°C, the numbers revealed that the URBACH energy is negatively proportional to the optical gap of the films at different heat temperatures. When spraying the film at a heat temperature of 400 C°, the electrical conductivity achieves a maximum of 0.0057/Cm, according to the Four Probe method study.

Keywords: Solar energy, Spray Pyrolysis, thin films, heat temperature, solar oven, X-Ray Crystallography, Ultraviolet–visible spectroscopy, Optical gap, Four Probe Technique, electrical conductivity, Nickel Nitrates.

Résumé

L'objectif de ce travail est d'utiliser l'énergie solaire pour produire des couches minces de nitrate de nickel (NiO) par la technique Spray pyrolyse, et d'étudier ensuite l'effet du changement de température sur les propriétés (structurelles, optiques et électriques), où Ni (NO3)2 6H2O a été utilisé, et de fines tranches ont été déposées sur des substrats de verre à concentration molaire (0,1 mol/l), tout en utilisant un four solaire à différentes températures (350, 375, 400, 425 et 450°C). Cette étude a été élaborée pour examiner les propriétés des lames minces en utilisant la technique de diffraction des rayons X (propriétés structurelles) et la spectroscopie des rayons. Ultraviolet et visible (propriétés optiques), ainsi que la méthode des quatre pointes (propriétés électriques). L'analyse aux rayons X a montré que nos échantillons cristallisent selon une structure cubique, les cristaux en lamelles adoptent une direction privilégiée selon la direction (1 1 1), où la dimension des grains atteint un maximum (37,7 nm) à une température (450°C) avec une diminution de l'épaisseur de la tranche. Alors que l'analyse UV-visible a montré que la transmittance de la tranche avait augmenté à une température (400°C). Le calcul a généralement montré que l'énergie URBACH est inversement proportionnelle au gap optique (Eg) des couches sous différentes températures. L'analyse par la méthode des quatre pointes a montré que la conductivité électrique (σ) atteint un maximum (0,0057 ohm 1-cm-1) lors de la pulvérisation de la lame à une température de (400°C).

Mots clés : l'énergie solaire - Spray pyrolyse - couches minces - température - four solaire - diffraction des rayons X - UV visible - gap optique (EG) - Méthode des quatre pointes - conductivité électrique - nitrate de nickel.

ملخص

الهدف من هذا العمل هو استخدام الطاقة الشمسية من اجل انتاج الطبقات الرقيقة لنترات النيكل (NiO) بواسطة تقنية الرش الحراري الشمسي، ثم دراسة تأثير التغيير في درجة الحرارة على الخصائص (البنيوية، الضوئية والكهربائية)، حيث استخدم Ni (NO3)2 6H2O وتم ترسيب الطبقات الرقيقة على ركائز زجاجية بتركيز مولي (0.1 مول / ل) وباستخدام فرن شمسي تحت درجات حرارة مختلفة (350 , 375 , 400 , 425 و450 درجة مئوية) .أجريت دراسة معاينة خصائص الطبقات الرقيقة بتقنية انعراج الاشعة السينية (الخصائص البنيوية)، ومطيافية الاشعة فوق البنفسجية والمرئية (الخصائص الضوئية)، وكذا طريقة المسابر الأربعة (الخصائص الكهربائية) .اظهر التحليل بالأشعة السينية ان عيناتنا تتبلور وفق بنية مكعبة، تعتمد بلورات الطبقات الرقيقة اتجاها مفضلا وفق الاتجاه (1 1 1)، حيث يصل بعد الحبيبات الى حد اقصى (37.7 نانو متر) عند درجة حراري (450 درجة مئوية) مع انخفاض سمك الطبقة .بينما اظهر التحليل بالأشعة فوق البنفسجية والمرئية ان نفاذية الطبقة قد ازدادت في درجة حراري (400 درجة مئوية)، وقد اظهر الحساب عموما ان طاقة URBACH تتناسب عكسيا مع الفجوة الضوئية المانعة (Eg) للشرائح في درجات الحرارة المختلفة .واظهر التحليل بواسطة تقنية المسابر الأربعة ان الموصلية الكهربائية(σ) تصل الى حد اقصى (0.0057 اوم 1- سم1-) عند رش الشريحة في درجة حرارة (400 درجة مئوية).

الكلمات المفتاحية: الطاقة الشمسية، الرش الحراري، الطبقات الرقيقة، درجة الحرارة، الفرن الشمسي، انعراج الاشعة السينية، الاشعة فوق البنفسجية المرئية، الفجوة الضوئية المانعة، تقنية المسابر الأربعة، الموصلية الكهربائية، نيترات النيكل.